Review

Ferritin: A Promising Nanoreactor and Nanocarrier for Bionanotechnology

Abhinav Mohanty, Akankshika Parida, Rohit Kumar Raut, and Rabindra K. Behera*

Cite This: *ACS Bio Med Chem Au* 2022, 2, 258−281

Read Online

ACCESS | Metrics & More | Article Recommendations

ABSTRACT: The essence of bionanotechnology lies in the application of nanotechnology/nanomaterials to solve the biological problems. Quantum dots and nanoparticles hold potential biomedical applications, but their inherent problems such as low solubility and associated toxicity due to their interactions at nonspecific target sites is a major concern. The self-assembled, thermostable, ferritin protein nanocages possessing natural iron scavenging ability have emerged as a potential solution to all the above-mentioned problems by acting as nanoreactor and nanocarrier. Ferritins, the cellular iron repositories, are hollow, spherical, symmetric multimeric protein nanocages, which sequester the excess of free Fe(II) and synthesize iron biominerals ($Fe_2O_3 \cdot H_2O$) inside their ∼5−8 nm central cavity. The electrostatics and dynamics of the pore residues not only drives the natural substrate Fe^{2+} inside ferritin nanocages but also uptakes a set of other metals ions/counterions during *in vitro* synthesis of nanomaterial. The current review aims to report the recent developments/understanding on ferritin structure (self-assembly, surface/pores electrostatics, metal ion binding sites) and chemistry occurring inside these

supramolecular protein cages (protein mediated metal ion uptake and mineralization/nanoparticle formation) along with its surface modification to exploit them for various nanobiotechnological applications. Furthermore, a better understanding of ferritin self-assembly would be highly useful for optimizing the incorporation of nanomaterials *via* the disassembly/reassembly approach. Several studies have reported the successful engineering of these ferritin protein nanocages in order to utilize them as potential nanoreactor for synthesizing/incorporating nanoparticles and as nanocarrier for delivering imaging agents/drugs at cell specific target sites. Therefore, the combination of nanoscience (nanomaterials) and bioscience (ferritin protein) projects several benefits for various applications ranging from electronics to medicine.
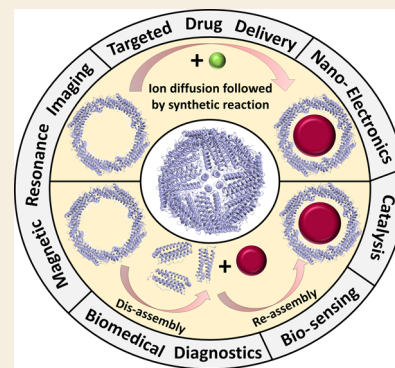
KEYWORDS: *Ferritin, Nanocage, Iron, Metal Ion Binding, Quantum Dots, Nanoparticles, Biomedical Applications, Nanotechnology*

1. INTRODUCTION

Bionanotechnology, derived from the fusion of basics of biotechnology and nanotechnology, covers multidisciplinary research related to the design and synthesis of biosensors, nanomaterials, and nanodevices toward biomedical and environmental applications.[1,2] Bionanotechnology helps to ease numerous challenges associated with life sciences by incorporating the cutting-edge innovations of nanotechnology into contemporary medical diagnostic issues.[3] Implementation of bionanotechnology in cellular imaging and drug delivery-based applications implies that the design of products/tools and the mechanism of actions should exhibit a high degree of cell/tumor specificity.[4,5]

Since the advent of the industrial revolution, the anthropogenic effect on the environment has expanded the degree of harmful heavy metal ions.[6−8] Heavy metals such as mercury, cadmium, lead, the metalloid arsenic, etc., known to pose serious threat to the living organisms, occur in different levels and in various chemical forms, with differential health consequences, thereby enhancing the rates of morbidity and

mortality.[9] Thus, heavy metal toxicity stands as a global problem, which needs to be solved either by sequestration or by detoxification. Both conventional (chelation therapy) and the emerging therapies (toxicogenomics and bioremediation) exist for sequestration/detoxification and are also successful to some extent but with some limitations.[10−13] Challenges also exist in the field of cancer diagnosis, in terms of limited bioaccessibility of imaging agents/drugs to tumor sites owing to their nonspecific targeting, thereby leading to inaccurate detection, reduced drug efficacy, higher dose requirements, and enhanced toxicity.[14−16]

Nanotechnology in the form of nanomaterials such as iron oxides, zinc oxides, titanium oxides, cerium oxides, zirconium

oxides, carbon and silica-based nanomaterials, etc. have emerged as a feasible solution to these problems but are commonly associated with the possibility of adverse health impacts caused by exposure to such different nanomaterials.[17−19] The potential risks include high toxicity, low biocompatibility, penetration/interaction with biological membranes/tissues, etc. Self-assembling proteins have emerged as a novel methodology for the creation and design of programmable nanomaterials that have proved to be highly efficient and effective by overcoming the limitations listed above.[20,21] Therefore, proteins and peptides have been utilized as smart building blocks and supramolecular templates for designing bioinspired nanomaterials exhibiting enhanced solubility and biocompatibility along with reduced toxicity, biodegradability, stability, surface modification/bioconjugation, ease of particle size control, targeted drug delivery, etc. Apart from providing interior compartments with nanoscale dimensions for synthesizing and incorporating nanomaterials (role as nanoreactor) with tunable physicochemical properties, these biomimetic materials act as nanocarriers by providing an efficient scaffold for encapsulation, controlled release, and site-specific targeted delivery of cargoes such as nanoparticles, enzymes, drugs, etc.[22−24]

Ferritin, the self-assembled protein nanocage, naturally stores iron and plays a crucial role in iron metabolism/homeostasis.[25−28] Cellular metabolism requires about micromolar to millimolar levels of iron for ATP/RBC/DNA synthesis and various enzymatic organic transformations such as oxidation and oxygenation reactions by tuning its redox properties.[26,29−32] However, the aerobic cellular environment and neutral pH oxidizes the iron and decreases its solubility ($\sim10^{-18}$ M) and bioavailability.[26,27] Therefore, its redox behavior is not only responsible for its essentiality but also for its toxicity and solubility.[33] To minimize its toxicity (Fenton's reaction) and enhance its solubility/bioavailability, nature uses ferritins which rapidly sequester and store the free/excess iron inside their inner cavity.[26,34] These proteins are ubiquitous in all tissues where their expression levels are regulated by cellular iron levels and in response to infection/inflammation (during oxidative stress). These proteins have a hollow, spherical shaped nanocage architecture possessing an external and internal diameter of ~12 and ~8 nm (in maxiferritin) and ~9 and $\sim4.5-5$ nm (in mini ferritin), respectively.[34−38] These nanocaged proteins formed from spontaneous self-assembly of identical or almost identical subunits (α-helical polypeptide chains) arranges into a highly symmetrical structure containing multiple pores/channels across its surface (Figure 1). Rapid sequestration (in a few milliseconds to seconds) of the labile, highly toxic free Fe^{2+} ions takes place through its hydrophilic pores/channels and are ferried to the ferroxidase centers (F_{ox}), where the oxidoreduction reaction takes place.[34,36,39−41] Finally, these ferric mineral precursors migrate toward the ferritin protein nanocavity for the formation of ferric (oxy)hydroxide ($Fe_2O_3 \cdot nH_2O$) mineral.[34,36,39] This protein encapsulation (cage) increases the solubility of these minerals and keeps them in a safe/nontoxic form and releases iron in a controlled fashion for cellular metabolism.[29−31] Thus, these iron storage and detoxification ferritin proteins play an important role during iron metabolism and host−pathogen interactions.[34,42] Moreover, some ferritins are exceptionally associated with DNA protection against oxidative stress (antioxidative activity).[26,34]
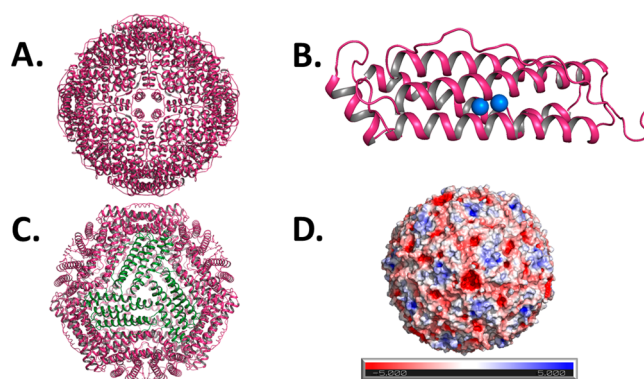
Figure 1. Structure and surface electrostatics of ferritin nanocage. A hollow, spherical shaped self-assembled ferritin nanocage consisting of 24 subunits viewed through (A) one of its six C_4 (4-fold) symmetry axes; (B) a single polypeptide subunit with the catalytic di-iron binding ferroxidase centers (F_{oxi}; represented as blue spheres in the middle of the subunit); (C) ferritin nanocage viewed through one of its eight C_3 (3-fold) symmetry axes; (D) the corresponding surface electrostatics of ferritin nanocage generated using PyMOL (PDB ID:1MFR), where negative, positive, and neutral amino acid residues are shown in red, blue, and white colors, respectively.

These protein cages are very stable, both thermally and chemically, being able to withstand extreme conditions such as high temperatures and excess concentration of denaturing agents.[27,37] Ferritin cages can reversibly disassemble (at low pH/high concentration of urea/GdnHCl) and reassemble (at high pH/low concentration of urea/GdnHCl). High stability, nanosized cavity, metal ion scavenging ability, and the reversible disassembly/reassembly behavior of ferritin cage have been largely utilized for the synthesis of nanomaterials and used in several biomedical applications in the form of nanocarrier, nanoenzymes, nanotheranostics, etc.[27,43−45]

In this review article, the current progress, recent significant developments, and ongoing efforts focusing on the self-assembling ferritin protein nanocage based nanoreactors and nanocarriers have been summarized. This review also highlights the prospects for future research on these natural, versatile promising protein assemblies in several fields ranging from catalysis to *in vivo* delivery systems.

2. STRUCTURE, FUNCTION, AND SELF-ASSEMBLY OF FERRITINS

Ferritins are $\sim450-500$ kDa hollow nanocages capable of incorporating up to ~4500 Fe atoms inside its protein nanocavity and store them in the form of ferric (oxy)hydroxide mineral.[26,39,41,44,46−53] The superfamily of ferritins is classified in three different types: the nonheme binding ferritins (Ftn), the heme-binding bacterioferritins (Bfr), and the Dps proteins (DNA-binding proteins from starved cells). Ftn and Bfr are maxi-ferritins (24-mers), whereas the Dps proteins are mini-ferritins (12-mers).[54−57] All the three subfamilies share the characteristic folding of 4 α-helical bundles. All the three domains of life (bacteria, archaea, and eukaryotes) synthesize Ftn proteins; Bfr proteins are specific to bacteria. Both Ftn and Bfr have identical quaternary structure, but the most significant difference between them is the presence of heme groups (up to 12 heme groups per cage) at the subunit dimer interface of Bfrs and the amino acid residues at/around the catalytic ferroxidase centers.[34,38,58−63]

Maxi-ferritins are hollow nanocage architectures formed spontaneously by the self-assembly of 24 subunits where each subunit is a polypeptide bundle made up of 4 α-helices and possess a catalytic site (ferroxidase center; F_{ox}) at the center along with a short helix toward the C-terminal.[64] These ferritin subunits undergo self-assembly in a 4−3−2 symmetry thereby creating eight 3-fold, six 4-fold, and twelve 2-fold pores/channels. The residues at/around these junctions are possibly crucial for the cooperativity in self-assembly, cage stability, and Fe^{2+} uptake/oxidation. The incorporated iron is stored in the internal cavity (∼8 nm) surrounded by a ∼2 nm thick protein shell, along with variable amounts of phosphate which vary among different organisms (Fe/P_i ∼1−2 in the case of plants/bacteria and >10 in the case of mammals).[27,36,65,66] Mammalian cytosolic ferritins are heteropolymers comprising of L-chain (light chain, 19 kDa) and H-chain (heavy chain, 21 kDa), where their ratio is tissue specific.[41,51,53,67−69] Although both the subunits (H and L) share a similarity in terms of sequence (∼55%) and folding, their functions are discrete. The H-chain possesses the F_{ox} center, which is crucial for rapid Fe^{2+} uptake, whereas the L-chain facilitates iron mineralization and stabilizes the iron mineral core inside the ferritin nanocavity.[41,67] In humans, although ferritin occurs as a coassembly of H- and L-chain subunits in a tissue-specific ratio, the mitochondrial ferritins comprise of only the H-chain. Although, serum ferritins are comprised of majorly L-chain subunits, but their origins are not well understood.[70] In contrast, "M" type subunits (middle) are specifically found in amphibians and closely resemble vertebrate H type (∼85% sequence identity). Prokaryotic and plant ferritins are composed of 24 identical/similar types of subunits, each having the catalytic ferroxidase center. Furthermore, the bacterial ferritins, along with 4−3−2 symmetry, comprise 24 asymmetrical pores called as B-pores, where one subunit dimer meets another in a side-on fashion.

The 12-mer mini-ferritins also self-assemble to form a cagelike architecture, similar to 24-mer maxi-ferritins, thereby creating six dimer interfaces at 2-fold symmetry axes and four 3-fold pores centered at the 3-fold axes but lack the C_4 symmetry axis (possibly due to the absence of the short fifth helix).[27,54−57,71] In addition, the ferroxidase sites are located at the dimer interface (2-fold axes). The external diameter of these Dps proteins is ∼8−9 nm with a central nanocavity of ∼4.5−5 nm, accounting to ∼20−25% of internal volume of maxi-ferritins and are capable of accommodating ∼500 Fe. Therefore, its primary function is iron detoxification (forms stable complex with DNA and protects the bacteria against oxidative damage) as opposed to iron storage in maxi-ferritins. These proteins also fold into a 4-helix bundle in a fashion similar to maxi-ferritins. Besides, Dps proteins have the capability to bind DNA, unlike maxi-ferritins (exceptions are some heme-binding Bfrs such as *M. tuberculosis* BfrA[34]).

The pores/channels formed from the self-assembly of subunits create favorable electrostatics along the 3-fold pores (in eukaryotic ferritins) and B-pores (in prokaryotic ferritins), which facilitates Fe^{2+} uptake inside the ferritin protein nanocage. Both the theoretical (electrostatics calculations) and experimental (site-specific mutagenesis and structural analysis by X-ray diffraction) studies of different ferritins established the role of hydrophilic 3-fold pores as the major Fe^{2+} uptake routes in eukaryotic ferritins. The inner cavity of ferritins is lined with acidic amino acid residues, which serve as iron nucleation sites and stabilize the iron mineral as well as

the non-natural metal oxide/hydroxide minerals.[72,73] However, the Fe^{2+} uptake routes in bacterial ferritins are less explored, in comparison to the eukaryotic ferritins. In recent years, it has been elucidated that the B-pore channels act as major Fe^{2+} entry pathways in *E. coli* Bfr (bacterioferritin), owing to the presence of acidic residues. Nevertheless, many aspects of Fe^{2+} translocation in ferritins from all domains of life are not fully comprehended, including the role of intrinsic self-assembly; whose disruption leads to complete/partial inhibition of catalytic activity in ferritins, despite having intact F_{ox} centers.

3. SEQUESTRATION OF IRON AND OTHER METAL IONS BY FERRITINS AND THEIR BINDING SITES

Synthesis of novel nanomaterials/particles inside the ferritin nanocavity with controlled size and morphology requires some prior information about the uptake of precursor metal ions (*via* nanoreactor routes; discussed later) and their interactions with ferritin protein. Similar to metal ion transport in transmembrane ion channels, the entry of various metal ions to the ferritin cages also occurs *via* its ion channels/pores (discussed in section 2). The favorable electrostatic gradient and dynamics of pore residues enable the uptake of iron and other non-native metal ions. The metal ion binding sites and their accumulation at the internal surface can be explained by geometrical preference of the corresponding metal ions, electrostatics, and hard and soft acids and bases (HSAB) theory. Similarly, these ferritin pores can uptake various metal complexes and small organic molecules with relatively slower rates as compared to the native (iron) and non-native (other) metal ions. The binding sites of these non-native metal ions in ferritin nanocage are briefly described in this review and the details can be found in some classic articles/reviews from various groups.[47,74−81]

This unique ability of ferritin protein has been exploited both by nature and researchers for the synthesis of various size-constrained nanoparticles (NPs), by using it as a nanosink, which has multiple advantages such as altered morphology/crystallinity and physicochemical (e.g., opto-electronic) properties. Moreover, the NPs synthesized within the ferritin nanocavity exhibit enhanced water solubility and biocompatibility/bioavailability, which can be exploited for diverse set of applications in nanotechnology, medicine, imaging, etc. For example, these encapsulated iron oxide NPs are used in magnetic resonance imaging (MRI), targeted drug delivery, and cell imaging,[82,83] whereas platinum NPs have mimicked excellent nanoenzymatic behavior, such as catalase and peroxidase activities.[84]

3.1. Fe^{2+} Uptake, Translocation, and Fe^{3+} Accumulation

Iron, being the natural substrate for ferritin, its uptake/translocation, initial stages of mineralization, and mineral core formation are investigated by different groups.[34,36,39,40,48−53,69,85−87] For eukaryotic ferritins, site-specific mutagenesis and X-ray diffraction studies have been carried out with human and frog M ferritins (mostly by Theil, Chasteen, and Harrison groups) and revealed the role of hydrophilic 3-fold pores for the sequestration of Fe^{2+}. The carboxylate side chains of Asp and Glu residues (D127 and E130) along the 3-fold pores are crucial for iron uptake,[39,40,67,85] while E136 and E57 (also called transit sites) are involved in the transfer of Fe^{2+} from 3-fold pores to the F_{ox} center for rapid catalytic activity. Deletion of these carboxylate residues resulted in inhibition of F_{ox} activity.

Table 1. Binding Sites of Iron and Other Non-Native Metal Ions in Ferritin Protein Nanocages

M^{n+} ion	ferritin (PDB ID)	binding location			refs
		3-fold pores	4-fold pores	other sites	
Fe^{2+}/Fe^{3+}	frog M ferritin (3RGD/3RBC)	E130	H169	ferroxidase center; E23, E58, H61, E103, Q137, D140 others; H54	46, 75
Mg^{2+}	frog M ferritin (3KA3)	T118, D127, E130, S131		ferroxidase center; E23, E58, H61, Q137, D140, E103 transit sites; E57, E136 others; H54	39, 40, 47, 110
Zn^{2+}/Ca^{2+}	human H-ferritin (2CEI)	E134, H118, C130	H173	ferroxidase center; E27, E62, H65, E107, Q141	74
Cu^{2+}	frog M ferritin (3RE7)	E130, H114, C126	H169	ferroxidase center; E23, E58, H61, E103 transit sites; E57, E136 others; H54	75
Co^{2+}/Mg^{2+}	frog M ferritin (3KA4)	E130	H169	ferroxidase center; E23, E58, H61, E103 transit sites; E57, E136 others; H54	39, 47
Pd^{2+}	horse spleen L-ferritin (2Z5P/2Z5Q)	H114, C126, E130		internal surface of the cage; C48, H49, E45, R52	103
Au^{3+}	human H-ferritin (3ES3)	H118	H173	internal surface of the cage; H57, H60, H65, C140	108
Au^{3+}	horse spleen L-ferritin (3H7G)	C126, H114		internal surface of the cage; G45, C48, H49, R52, M96, H147	104
Ag^{2+}	Pyrococcus furiosus (2JD7)		M153	within the 4 α-helix; M170, H53, D49, E130	81
Ir^{3+}	recombinant horse liver L-ferritin			internal surface of the cage; C48, H38/H52	99

Moreover, the size of these 3-fold pores is also critical for rapid Fe^{2+} uptake, as revealed by E130D modification.[39,40] The role of 3-fold pores in Fe^{2+} entry was indirectly revealed when frog M ferritin was cocrystallized with redox inactive Mg^{2+} ions, where a line of Mg^{2+} ions were observed in the 3-fold channel, which was further linked to the F_{ox} center.[47] This investigation established the journey of Fe^{2+} inside the ferritin protein nanocage. Later, these observations were directly proved via a series of high-resolution X-ray diffraction data sets by freezing frog M ferritin crystals at different time intervals after exposure to Fe^{2+} salts.[75,88] As discussed above, the 3-fold pores are the potential gateway for the entry of many metal ions especially in eukaryotic ferritins, which was further corroborated by molecular dynamics simulations.[89−91] After Fe^{2+} acquisition/ferroxidase activity, mineral precursors undergo a series of complex hydrolytic reactions to synthesize ferrihydrite mineral inside the protein nanocavity, where a set of carboxylate residues (Table 1) stabilize this ferric (oxy)hydroxide mineral by electrostatic interactions[25,41,51,92] and possibly regulate the total iron accumulation.

Similarly, in case of bacterioferritins, MD simulation studies suggested that the thermal fluctuations of 4-fold and B-pores regulate the transport of monovalent cations via B-pores.[93,94] In addition, site-specific substitutions at the B-pore residues resulted in the inhibition of F_{ox} activity in E. coli Bfr.[58] However, further studies on the Fe^{2+} uptake pathways and translocation mechanisms in bacterial ferritins need to be carried out. Iron trafficking in mini-ferritins occurs via the "ferritin-like" 3-fold pores.[54−56]

3.2. Accumulation of Non-Native Metal Ions

Similar to iron accumulation, the incorporation of other divalent and non-natural metal ions inside the ferritin nanocavity under in vitro conditions are also observed at/along the ion channels/pores or at the internal surface in addition to the ferroxidase centers (Table 1). This has raised a fundamental question regarding the selectivity of ferritin toward iron, in vivo. It has been previously established that divalent metal ions, such as Cu^{2+}, Co^{2+}, Zn^{2+}, and Mn^{2+}, can compete with Fe^{2+} and significantly reduce the ferroxidase activity (solution kinetics)[37] by binding either at the 3-fold pores or at the ferroxidase centers (X-ray crystal structures).[39,44,47,49,74,79] The extent of inhibition of ferroxidase activity in the presence of these divalent metal ions can be explained based on the Irving−William series; Cu^{2+} and Zn^{2+}, which are known to form stable complexes exhibited maximum inhibition of F_{ox} activity. Cu^{2+} ions not only bind at the 4-fold pores but also to a C126 residue along with His and Glu[95] residues located at the 3-fold and is corroborated by the appearance of a Cu−S charge transfer band in solution.[39]

Similarly, X-ray crystallographic studies on frog M and human H ferritin indicated that the His residues near the 4-fold pores bind to the metal ions, such as Zn^{2+}, Cu^{2+}, Co^{2+}, Mn^{2+}, and Mg^{2+}, forming an octahedral geometry[95] (Table 1). However, Ag^{2+} binds to M153 (soft site) at the 4-fold pore of Pyrococcus furiosus ferritin also in a square planar geometry.[95] In addition, it also binds to several other residues present within the four helices such as M170, H53, D49, and E130. Moreover, introduction of His residues at the C_2 dimer interface yields a tetrahedral Cu^{2+} coordination, which can induce the metal-mediated ferritin self-assembly from its as-isolated monomeric form.[96] Further, the effective binding of Tb^{3+} ions at the 3-fold pores and the ferroxidase sites have been exploited for cell imaging and can be delivered into the tumor cells.[97] Moreover, these supramolecular ferritin nanocages have been successfully utilized for detoxification of heavy metal ions.[98] The binding and accumulation of Pd^{2+} and Au^{3+} in ferritin are discussed separately in the following section. A recent article by Taher et al. also investigated the impact of engineering the ferritin protein nanocages, where the site-specific mutations of two polar residues (D38 and R52) by His residues near the dominant Ir^{3+} binding sites (C48) influenced the enhancement of IrCp* uptake inside the protein nanocages to design hybrid biocatalysts for carrying out the transfer hydrogenation reaction of various aromatic carbonyl compounds.[99]
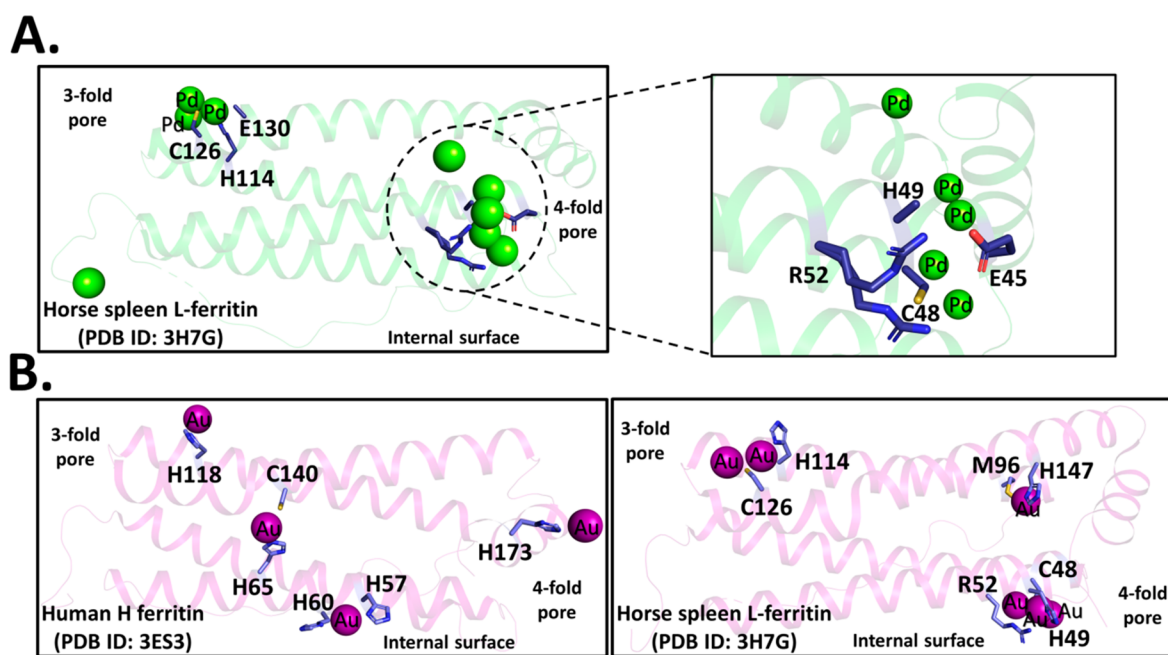
Figure 2. Binding sites for (A) Pd^{2+} and (B) Au^{3+} in ferritin protein nanocages.

3.2.1. Pd^{2+} Accumulation. Palladium NPs have found great attention in the field of catalysis, sensing, and hydrogen storage, etc.[100] In recent years, Pd NPs have been synthesized inside the nanocavity of horse spleen L-ferritin and have been used for catalytic applications.[101,102] The advantage of growing these nanoclusters within a confined space offers the ability to tune the physicochemical properties by regulating the size. Here, Pd^{2+} ions enter the ferritin cage possibly through the nanoreactor route (3-fold pore) as these metal ions were reported to interact with H114, C126, and E130 (Table 1 and Figure 2A) but accumulate relatively less Pd^{2+}, as compared to iron, at the internal surface of the ferritin cage.[103] Pd^{2+} ions exhibited its preferred coordination geometry (i.e., square planar) by binding with the C48/E45 residues, whereas the metal ions like Cd^{2+}, Fe^{2+}/Fe^{3+}, and Mn^{2+} form octahedral geometry. Using these accumulation properties of Pd^{2+} ions, bimetallic complexes of Au/Pd nanoparticles have been synthesized, which exhibited enhanced catalytic hydrogenation of acrylamide derivatives.[104] The substitution of H114 with Ala resulted in the construction of new metal binding sites (dinuclear to trinuclear complex) indicating that multinuclear complexes can be prepared by the deletion or introduction of metal ion binding sites on the protein surface.[103]

3.2.2. Au^{3+} Accumulation. Apo-ferritin nanocages have been used for the synthesis of water soluble and biocompatible gold nanoparticles having applications in the field of catalysis, biomedicine, and imaging.[101,104−107] Advancements in the field of Au nanoparticle were achieved by synthesizing them inside the ferritin nanocavity and were investigated with the help of a series of spectroscopic studies and have been used for *in vivo* kidney targeting and biomedical imaging.[107] Structural analysis of Au^{3+} ions with human H-ferritin (ferritin crystals soaked in solution of Au^{3+} ions) indicated its interaction with H65 and generated Cys residues[108] (Table 1 and Figure 2B, left). In addition, Au^{3+} ions also bind to four His residues, forming a square planar geometry, at the 4-fold pore. Further, the immobilization of Au^{3+} ions in horse spleen L-ferritin was investigated by Ueno and co-workers, where the Au atoms

were observed to bind selectively with sulfur containing amino acids (soft sites) C126 at the 3-fold pores and C48 and M96 at the internal surface of the cage[76] (Table 1 and Figure 2B, right). Further, site-specific mutagenesis was employed to introduce Cys residues (E45C/R52C) in order to enhance the accumulation of Au^{3+} ions.[109] These studies on Au binding in ferritin nanocage have potential in stabilizing small gold nanoclusters in protein scaffolds.

4. BIOMEDICAL AND BIOTECHNOLOGICAL APPLICATIONS OF FERRITINS: AS NANOREACTOR AND NANOCARRIER

4.1. Biocompatible Quantum Dots Encapsulated within Ferritin

4.1.1. Introduction to Quantum Dots. Quantum dots (QDs), also termed as nanocrystals or zero dimensional (0-D) nanoparticles (i.e., all the three dimensions are within the nanoscale regime, typically <100 nm), have gained considerable importance in recent times owing to their unique size dependent optical and electronic properties.[111−113] QDs can be basically defined as the fluorescent semiconductor nanocrystals which are composed of atoms of group IIB-VIA elements (such as CdS, ZnSe, ZnS, etc.) or group IIIA-VA elements (such as InP, GaAs, InAs, etc.) in the periodic table.[111,114,115] The name "quantum dots" is a combination of two terms derived from the properties of such crystals: "dots" referring to the nanoscale dimension (typical size ranges from 2 to 10 nm) of these particles while "quantum" term derives from the fact that these nanomaterials can be considered as a particle in a sphere (analogous to a particle in a box), which obeys all of the quantum mechanical principles.[113,116,117]

The elemental composition of these nanocrystals accounts for their semiconducting properties arising from the presence of a filled valence band and an empty conduction band generally with a band gap of less than ~3.4 eV.[111,113,118] Upon absorption of photons/during the conduction of electric currents by these semiconductor nanomaterials, the excita-

tion/promotion of electrons from the valence band to the conduction band leads to the formation of holes in the valence band, and this newly generated electron−hole pair constitutes an exciton possessing an exciton Bohr radius ($a_b{}^*$), equivalent to the average distance between the electron and hole, as defined by eq 1:

$$a_b{}^* = \varepsilon_r \left(\frac{m}{\mu} \right) a_b \tag{1}$$

where ε_r = size dependent dielectric constant (relative permittivity), m = mass of exciton, μ = reduced mass of exciton, and a_b = Bohr radius (0.53 Å). In analogy to the quantum mechanical solution of particle in a 1-D box model,[117,119] the energy levels of the exciton, also known as confinement energy, can be defined by eq 2, which depends on the size of the QDs:

$$E_{confinement} = \frac{\hbar^2 \Pi^2}{2a^2} \left(\frac{1}{m_e} + \frac{1}{m_h} \right) = \frac{\hbar^2 \Pi^2}{2\mu a^2} \tag{2}$$

where a = radius of the QDs, m_e = mass of free electron, m_h = mass of hole, μ = reduced mass. Furthermore, owing to the columbic attractions between the negatively charged electrons and the positively charged holes, the bound exciton energy term arises, which is directly proportional to Rydberg's energy (R_y) and inversely proportional to the size dependent dielectric constant, given by eq 3:

$$E_{exciton} = -\frac{1}{\varepsilon_r{}^2} \left(\frac{\mu}{m_e} \right) R_y = -R_y{}^* \tag{3}$$

Therefore, the total energy associated with the QDs is the total of the band gap energy, confinement energy, and bound exciton energy, which can be summarized as shown in eq 4:

$$\begin{aligned} E &= E_{bandgap} + E_{confinement} + E_{exciton} \\ &= E_{bandgap} + \frac{\hbar^2 \Pi^2}{2\mu a^2} - R_y{}^* \end{aligned} \tag{4}$$

The phenomena of quantum confinement experienced by these excitons can be categorized as strong, intermediate, and weak confinement depending upon whether the radius of the QDs is smaller than the exciton Bohr radius, smaller than the Bohr radius of either the electron or hole and not both, or greater than the Bohr radius of both electron and hole, respectively.[120,121] The emission properties of these nanomaterials are governed by their band gap which ultimately gets affected by the dimensions of the QDs, as stated by the Brus equation (eq 5),

$$E_{bandgap} = E_{bulk} + \frac{h^2}{8R^2} \left(\frac{1}{m_e{}^*} + \frac{1}{m_h{}^*} \right) - \frac{1.8e^2}{4\pi\varepsilon_0\varepsilon_r R^2} \tag{5}$$

where $E_{bandgap}$ = band gap energy of QDs, E_{bulk} = band gap energy of bulk semiconductor, R = radius of the QD, $m_e{}^*$ = effective mass of the electron, $m_h{}^*$ = effective mass of the hole, h = Planck's constant, ε_0 = permittivity of the vacuum, and ε_r = the relative permittivity. Band gap of the QDs increases with the decrease in size of these nanocrystals leading to a red shift in their emission spectral profiles, thus allowing one to fine-tune their optical and electronic properties as per the requirement of several applications in the field of nano-

technology, nanoelectronics, and nanobiotechnology.[112,114,122,123]

4.1.2. Synthesis and Properties of Quantum Dots.

Earlier techniques of QDs synthesis mostly involved the addition of stabilizing agents to the aqueous solutions of the precursor salts resulting in low-quality QDs exhibiting poor fluorescent properties and non-uniform size distributions.[111,118] The modern procedures mostly utilized the application of high temperature on organometallic precursors, which only resulted in the formation of monodispersed particles while no increase in the fluorescence efficiencies were observed with lower quantum yields (∼10%).[125] Enhancement in the quantum yield to nearly 40−50% was achieved by the surface capping of QDs such as ZnS capped CdSe QDs where an epitaxial growth of a layer of wider band gap QDs such as ZnS was observed over the surface of CdSe.[126−128] Overall, the size and subsequently the optical and electronic properties of these nanostructures can be controlled by regulating the temperature and the amount of limiting reagents.[129,130] The size tunable optical property along with the presence of multiple electronic states at higher energy levels allow the simultaneous excitation of multicolor QDs utilizing a single light source[124,131,132] (Figure 3). The emission

Figure 3. Size dependent optical properties of CdSe@ZnS core−shell QDs excited with a near UV lamp. (From left to right) A gradual bathochromic shift in the emission maximum (443−655 nm) was observed with the increase in size of QDs. Reproduced with permission from ref 124. Copyright 2001 Springer Nature.

wavelength can be tuned from blue to near-infrared regions of the electromagnetic spectrum with CdS, ZnSe QDs absorbing in the blue to near UV region, while InP, GaAs QDs absorb in the far red to near-infrared regions.[133,134] These optical properties provide additional advantages to QDs over the toxic organic dyes (such as Fluorescein, Rhodamine 6G, etc.) which were used for several bioimaging processes in terms of greater stability, significant brightness, and reduced rates of photobleaching.[135−137] Surface chemistry of such particles is also highly interesting since the solubility of these nanocrystals can be enhanced by surface coordination to various inorganic as well as organic molecules.[138−140]

4.1.3. Applications and Limitations of Quantum Dots.

The prospects of bioconjugation is another highly useful aspect of QDs in the field of biomedical applications since the protein coated QDs (covalent conjugation with various biomolecules owing to the presence of various functional group residues such as carboxylates, amines, etc.) exhibits excellent spectral widths, enhanced stability, and quantum yields.[141−143] Thus all such properties describe the reason behind the use of QDs in a large number of applications such as solar cells,[144] LEDs and lasers,[145,146] quantum computations,[147] biosensors,[148] in vivo molecular imaging,[149] DNA hybridization,[150] screening of drug

molecules,[151] real time tracking of growth of tumor cells,[152,153] etc. QDs are promising candidates for several applications in the field of biophotonics such as optical imaging,[154] photoacoustic imaging,[155] biosensing,[156] optical tracking,[157] photothermal therapy,[158] multimodal imaging,[159] etc. and even in the field of nanomedicine such as cancer nanotechnology,[160] *in vitro* diagnosis of infectious diseases,[161] protein and peptide delivery,[162,163] drug delivery,[164] imaging guided surgery,[165] gene delivery,[166] etc. (Figure 4).
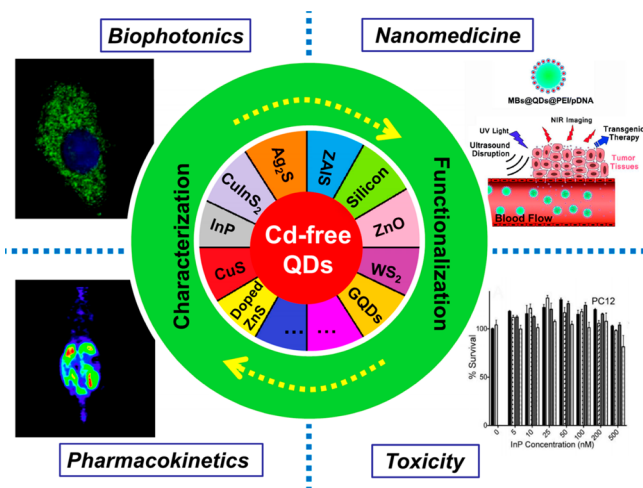
Figure 4. Potential applications of Cd-free QDs. Reproduced with permission from ref 153. Copyright 2016 American Chemical Society.

Despite their advantages/applications, one cannot deny the fact that most of these QDs are constituted from toxic elements such as cadmium, lead, etc.[167,168] Toxicity remains a major concern while using such QDs in biological systems since the stability gets affected to some extent by pH changes, oxidizing/reducing environment, etc. leading to the leaching/ release of toxic metal ions that can harmfully interact with the biomolecules to inhibit the normal cellular activities.[169−171]

4.1.4. Encapsulation of Quantum Dots by Ferritin. As stated above, the poor biocompatibility and the possible release/leakage of toxic ions into the biological system constitutes a major limitation in the use of these highly promising QDs for biomedical applications. The coating of these QDs by ferritin protein nanocages have successfully emerged as a possible solution to all the above-mentioned problems.[172−174] High thermostability, solubility, biocompatibility, metal ion scavenging abilities, and reversible self-

assembly nature of ferritin protein nanocage makes them highly suitable candidates to synthesize/load these nanomaterials (as nanoreactor) and to deliver them at the desired target sites (as nanocarrier).[26,27,43]

4.1.4.1. Via Nanoreactor Route. Xing et al. have successfully reduced the toxicity of CdSe QDs by encapsulating them within the apoferritin shell.[175] Apoferritin (AFt), the ferritin protein without the mineral core, are the protein shell having an outer diameter of ∼12 nm dimension with an internal cavity of ∼ 8 nm dimension and can serve as an excellent coating material for nanodimensional QDs.[27,37] The work involved the synthesis of CdSe QDs inside the ferritin cavity without disassembling the protein nanocage by incubating the AFt with the precursor ions: Cd^{2+} and Se^{2-}, which flowed into the protein shell through the hydrophilic channels followed by their quick reaction and formation of CdSe QDs (Figure 5).[175]

EDTA was also used to slow down the reaction, to prevent severe aggregation, and to remove excess of Cd^{2+} ions by forming a Cd(II)-EDTA complex. The UV−vis spectrum of the resulting AFt-CdSe QDs displayed absorption bands consistent with the bare CdSe QDs while the TEM images clearly confirmed the nanosize of QDs encapsulated by the intact protein shell. The photoluminescence spectrum also was in accordance with the bare QDs while the cytotoxicity studies performed on human cancer cell lines and human hepatocarcinoma cell lines demonstrated reduced toxic effects due to the protein shielding. All these results are clearly stating the fact that QDs retained all its optical properties, and the protein shell just served as a protective coating that reduced the toxic nature of CdSe QDs by preventing the possible leakage/release of harmful Cd^{2+} ions.[175]

Similarly, Bradshaw et al. have utilized AFt shell as a biotemplate for synthesizing PbS QDs, which not only exhibited excellent photoluminescence but also provided selective imaging and enhanced antitumor activity against human colorectal carcinoma.[176] Furthermore, the successful size constrained one-pot synthesis of QDs such as CdS, ZnSe, ZnS, etc. inside ferritin enhancing the biocompatibility, solubility, and stability of these nanomaterials opened up a wide range of possibilities for their utilization in nanomedicine, nanoelectronics, and nanobiotechnology.[177−181] Naito et al. have employed a similar approach to synthesize CdS QDs inside the shell of horse spleen ferritin.[182] The presence of patches of Glu/Asp residues at the interior surface of the ferritin not only provides the favorable electrostatics to promote the flow of precursor ions inside the protein cage
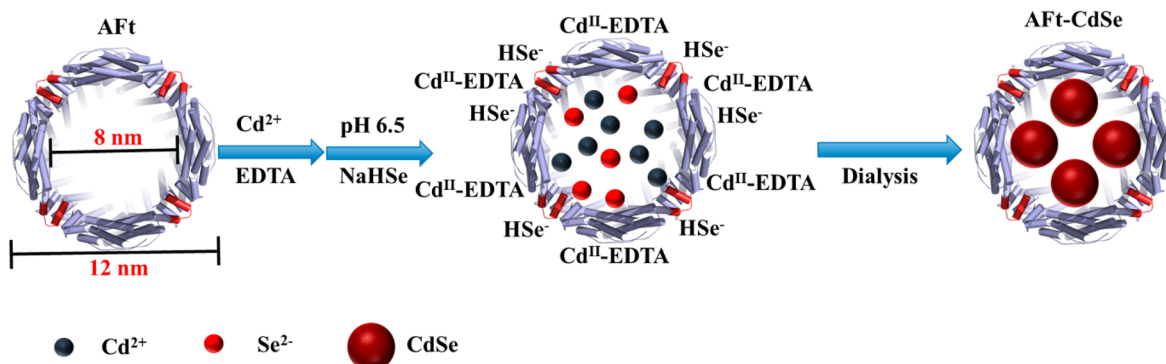
Figure 5. Schematic representation for the synthesis of CdSe QDs inside the apoferritin cavity *via* the nanoreactor route.

but also leads to the formation of CdS nanocrystals.[182] The hollow chiral protein served as a template for the synthesis of chiral QDs exhibiting circularly polarized luminescence (CPL) activity, which is highly useful for sensory biomedical applications.[182]

The AFt shell acted as a nanoreactor by synthesizing size constrained QDs inside its shell, mimicking the natural iron biomineralization process inside it. Moreover, it also provides the opportunity to conjugate other biomolecules on its surface, to exploit them in bioimaging and targeted drug delivery.[26,27,37,43] Furthermore, site directed mutagenesis could be employed to modify both the external and internal surfaces of ferritin depending upon the requirements/applications.[27]

4.1.4.2. Via the Disassembly/Reassembly Route. The group IIB-VIA semiconducting QDs such as CdS, ZnSe, and CdSe emit in the UV−visible regions of the spectrum (∼200−800 nm).[183] Therefore, applications of these QDs in deep tissue imaging is mostly limited.[184] On the other hand, group IVA-VIA nanocrystals such as PbS QDs provide efficient emissions at larger wavelengths (>1000 nm) but the problem of toxicity and water solubility limits its usage.[185,186]

Therefore, to decrease the toxicity and enhance the solubility, Hennequin et al. have synthesized near-infrared (NIR) fluorescent nanocomposites of PbS QDs inside the soluble horse spleen ferritin protein nanocage by adopting a pH dependent unfolding/refolding technique (Figure 6).[187]
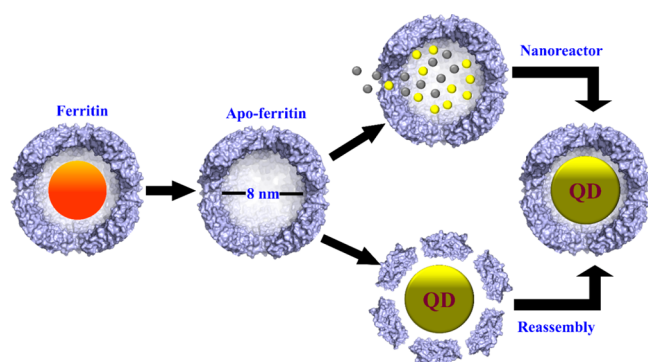
Figure 6. Scheme for formation of PbS@AFt composites *via* both the nanoreactor route and the disassembly/reassembly route.

In addition to the nanoreactor route described in the earlier section where the AFt was incubated with precursor Pb^{2+} and S^{2-} ions, which led to the formation of PbS QDs inside the protein nanocage, an alternative route (disassembly/reassembly of ferritin) was also used by Turyanska et al. to encapsulate PbS QDs inside horse spleen ferritin.[186] In this technique, these QDs were first synthesized using reported methods and then encapsulated within the protein nanocage. Horse spleen ferritin protein nanocage was first demineralized (removal of iron mineral) to form an AFt shell by thioglycolate treatment followed by repeated dialysis against NaOAc buffer until the ferritin solution got decolorized.[187,188] The pre-synthesized QDs were encapsulated by disassembling AFt protein nanocages at pH 2 and then reassembling it at pH > 5 to incorporate PbS QDs. The crystal structure and the optical properties of encapsulated PbS QDs remained unaltered during this pH dependent unfolding/refolding process. High-resolution transmission electron microscopy (TEM) images revealed the hexagonal closed packed structure of AFt-PbS nanoparticles with EDX spectrum confirming the presence of

Pb and S inside the intact protein shell, which are also supported by their native polyacrylamide gel electrophoresis (PAGE) profile. Cytotoxicity studies (MTT assay) on nontumorigenic and carcinoma cells illustrated that the toxicity levels of protein encapsulated QDs were significantly lower as compared to the bare ones. These results suggested that the optical properties of encapsulated PbS QDs were hardly affected by the protein shield, which ultimately enhances their solubility and reduces their toxicity as compared to the commercially available/synthesized bare QDs. Different research groups have implemented the nanoreactor route and/or disassembly/reassembly approach for incorporating different QDs such as CdS, PbS, ZnSe, CdSe, and carbon based QDs inside ferritin protein nanocages for various bionanotechnological applications and are enlisted in Table 2. Apart from the two routes (nanoreactor and the disassembly/reassembly approach) mentioned so far for the encapsulation of QDs inside ferritin, Nasrollahi et al. have utilized a unique metal (Fe) ion dependent self-assembly of *Archaeoglobus fulgidus* ferritin to incorporate graphene QDs along with the drug doxorubicin for dual utilization as a bioimaging agent and drug nanocarrier for breast cancer diagnosis.[189]

4.1.5. Synthesis of Apoferritins for Enhancing Photoluminescence of Ferritin Encapsulated Quantum Dots.

Owing to the toxicity of the conventional Cd/Pb-based QDs,[167,184] the need for cadmium/lead-free QDs have led to the development of nontoxic QDs such as carbon dots (C-dots),[190] silicon dots (Si QDs),[191] Ag_2S/Ag_2Se QDs,[192,193] etc. Si QDs are highly biocompatible and have been successfully utilized in various cancer-related bioimaging purposes.[191] Similarly, carbon dots are an effective replacement for the toxic QDs, since the biocompatibility and low toxicity are additional assets apart from their excellent optical and electronic properties.[153,194]

However, utmost care must be implemented while synthesizing/incorporating such fluorescent nanomaterials inside ferritin, since the majority of the works involving ferritins and QDs have utilized commercially available horse spleen ferritin (Table 2), which are mostly mineralized (loaded with ∼2000 iron per cage). The presence of Fe^{3+} ions in the iron mineral core of ferritins quenches the photoluminescence (PL) of QDs *via* static electron transfer from the QDs to the vacant d-orbitals of Fe^{3+} inside the protein nanocage, thereby reducing the efficiency of QDs as fluorescent probes/sensing/imaging agents.[195] Bhattacharya et al. have reported such PL quenching of C-dots by equine spleen ferritin, where the PL of C-dots was quenched by nearly 2.7 times in the presence of ferritins, whereas no such quenching was observed in the case of apoferritin, clearly indicating the role of Fe^{3+} of the mineral core in the quenching process.[195]

Although ferritins are demineralized in most of the reports involving the synthesis/incorporation of QDs, even the traces of Fe^{3+} present inside ferritin may affect the PL intensities.[195] Therefore, these ferritin samples first need to be demineralized thoroughly to remove all the iron content loaded inside them in order to generate their apoforms. The demineralization of ferritin protein is usually performed by treatment and/or extensive dialysis of the mineralized ferritin samples with buffer solutions containing reducing agents such as thioglycolic acid, thioacetic acid, sodium dithionite, dithiothreitol, etc. to reduce the iron mineral core, under a N_2 environment, followed by the chelation of iron(II) using suitable chelators such as ferrozine,

Table 2. Encapsulation Routes and Applications of Ferritin-QDs Nanomaterials

type of ferritin	mineral core (QDs)	core size (nm)[a]	encapsulation route	applications and proposed applications	refs
horse spleen ferritin	CdS	2.5−4.0	nanoreactor	tunable photochemical agents for cancer diagnosis, sensing of heavy metal ions, and targeted drug delivery.	177
horse spleen ferritin	PbS		nanoreactor and pH-based disassembly/reassembly	noninvasive fluorescence imaging and therapeutic tissue targeting	186
horse spleen ferritin	CdSe	4.2	nanoreactor	enhanced solubility and biocompatibility, reduced cellular toxicity	175
equine spleen ferritin	carbon dots	<2	size dependent penetration	optoelectronic and bioimaging applications	195
horse spleen ferritin	CdS	6.0−7.1	nanoreactor	tunable circularly polarized fluorescence, chiroptical memory, emitting devices	182
horse spleen ferritin	PbS	6 ± 2	nanoreactor and pH-based disassembly/reassembly	enhanced solubility and biocompatibility	187
horse spleen ferritin	CdSe	6.0 ± 0.6	nanoreactor	pathway to synthesize uniform II-VI semiconductor nanoparticles for biomedical and nanoelectronics applications	178
horse spleen ferritin	PbS		nanoreactor and pH-based disassembly/reassembly	antitumor activity against colorectal carcinoma cells	176
horse spleen ferritin	PbS	6.0−6.7	nanoreactor	photovoltaics	197
Archaeoglobus fulgidus ferritin	graphene QDs with ferrihydrite	2.8 ± 0.8	metal mediated self-assembly	pH-responsive fluorophore, MRI agent, and drug nanocarrier	189
horse spleen ferritin	ZnSe	3−7	nanoreactor	biotemplate for synthesis of semiconductor NPs	181
horse spleen ferritin	CdS	4.7−7.1	nanoreactor	nanoelectronic devices or fluorescent biomarker	180

[a]Determined from TEM analysis.

2,2′-bipyridyl, etc.[31,38,196] Therefore, the resultant apoferritin samples can be utilized as a biotemplate for synthesizing/incorporating a wide variety of QDs whose PL properties would not get compromised.

4.2. Ferritin in Nanomaterial Synthesis and Bionanotechnology

4.2.1. Synthesis and Applications of Nanoparticles.
The synthesis of nanoparticles, particularly superparamagnetic iron oxide nanoparticles (SPION), hold crucial significance owing to its various applications including hyperthermia-based cancer treatment,[198] gene therapy,[199] targeted drug delivery,[200] MRI contrast agents,[201] among several others. However, the critical size of such nanoparticles are required to be smaller than 100 nm, typically as low as 10−20 nm or even of the lower order for effective functioning/activity in majority of these applications.[202,203] Earlier reports have suggested the origin of the superparamagnetic nature in iron oxide nanoparticles to be the ultrasmall size and the narrow particle size distribution responsible for the individual magnetic domain behaving as "single super spin".[204,205] Such nanoparticles have been reported to exhibit high values of magnetization and magnetic susceptibility, whereas their retentivity and coercivity remain relatively low. Under the influence of external magnetic field, these particles can be utilized for the treatment of malignant tissues/organs owing to their easy binding and bioconjugation to proteins, drugs, and antibodies for targeted delivery applications.[206,207] Nevertheless, the agglomeration of such nanoparticles owing to their high surface area to volume ratio, which compels them to reduce their energy *via* aggregation, emerges as one of the major limitations in their usage and applicability. Therefore, efforts have been made to stabilize the nanoparticles by employing various protection strategies in the form of organic or inorganic layer coatings,[208,209] surfactant or polymer coatings,[210,211] or biomolecular templating,[212,213] etc. Earlier reports have suggested the use of biomolecule-based supra-

molecular templates which are both genetically and chemically modified with metal binding ligands for the synthesis of stable, monodispersed encapsulated nanoparticles. The risk of aggregation gets considerably reduced in such functionalized nanoparticles, thereby accounting for their availability in wide range of applications ranging from catalysis to biosensing applications[204,205] (Figure.7). Among the commonly used magnetic nanoparticles, both magnetite (Fe_3O_4) and maghemite (γ-Fe_2O_3) exhibit a transition in their magnetic behavior from ferromagnetic to superparamagnetic upon reduction in
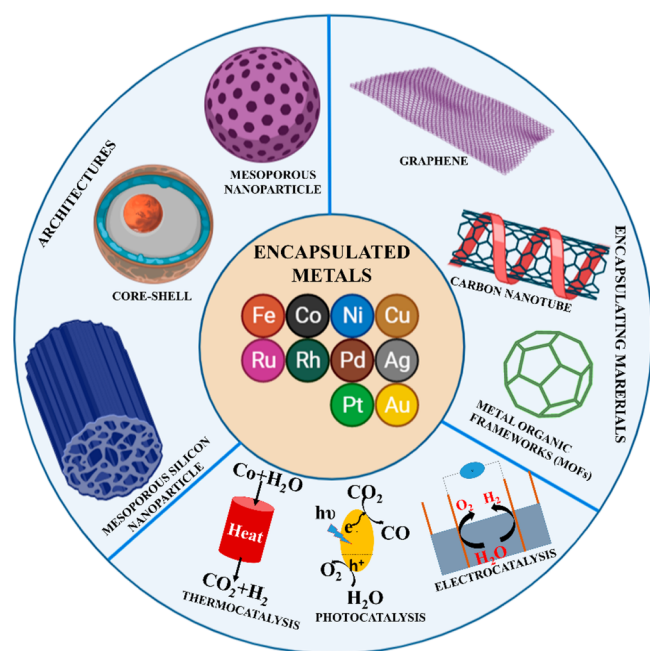
Figure 7. Different sets of nanoparticles along with their architectures, encapsulating scaffolds, and applications.

their sizes (<20 nm) leading to a loss of their permanent magnetism.[214] Other metallic and metal hydroxide/oxyhydroxide nanoparticles hold potential biomedical applications, but problems such as solubility, toxicity, and harmful interactions with membranes and tissues other than target sites is a cause of major concern and often restricts their usage.[215,216]

In order to utilize the nanoparticles for various biomedical applications, several synthetic strategies have been utilized for the preparation of highly stable and monodispersed nanoparticles such as hydrothermal synthesis,[217] the laser pyrolysis technique,[218] the coprecipitation method,[219] thermal plasma synthesis,[220] the sol–gel method,[221] etc. among several others. Among all the listed chemical pathways for nanoparticle synthesis, coprecipitation method can be termed as one of the simplest and most effective routes which generally involves chemical reaction between stoichiometric mixture of precursor salts in aqueous/organic mediums, followed by the addition of a base/alkali, at elevated or room temperature.[219] The major advantage of this approach is the high yield obtained as a result of the production of large quantity of nanoparticles. Reaction conditions such as pH of the medium and reaction temperature plays a vital role in modulating the mean size of the particles.[222] However, the major disadvantage associated with the coprecipitation technique is the inability to control the particle size owing to extensive agglomeration. Another synthetic approach involves the utilization of organic solvents having high boiling points in combination with suitable surfactants for carrying out the thermal decomposition of organometallic precursors under high temperature conditions leading to the formation of nanoparticles.[223] Variation in the experimental parameters such as ratios of starting materials, reaction time duration, and temperature governs the size and morphology of the synthesized nanoparticles.[224] Moreover, reduction in the chain length of fatty acids used as surfactant has been reported to have a positive impact on the reaction rate. On the other hand, the adsorption of surfactant on the surface of the synthesized nanoparticles accounts for their stability.[225,226]

Alternatively, a wet chemical synthetic approach known as the sol–gel technique has proven to be highly beneficial owing to high chemical homogeneity and low cost associated with the preparation of metal oxide nanoparticles.[221] These reactions are generally carried out at room temperature but are subsequently subjected to heat treatments at different phases of the reaction to develop the nanocrystalline structure while the size of such nanoparticles gets regulated by the annealing temperature.[227] Moreover, functionalization of the synthesized nanoparticles can be carried out by further embedding them into the silica matrix.[228] Thermal plasma is another synthetic route for the preparation of nanoparticles where vapors of organometallic precursor compounds such as $Fe(C_5H_5)_2$, $Fe(CO)_5$, $Fe_3(CO)_{12}$, etc. along with oxygen gets inserted into an argon DC thermal plasma leading to their evaporation and recondensation.[229] As discussed earlier in the case of previous synthetic routes, the size and morphologies of nanoparticles get regulated with the oxygen flow rate during the reaction.[230] The iron oxide nanoparticles obtained via the thermal plasma technique have been reported to exhibit high saturation magnetization values.[231]

Another technique that has been reported to be highly useful for the large-scale generation of nanoparticles is the spray pyrolysis technique which exhibits high temperature-based solvent evaporation and solute condensation during the course

of the reaction featuring the spraying of a solution of metal precursor salts and a reducing agent into a series of reactors.[232,233] Similarly, laser pyrolysis technique makes use of laser to heat a mixture of precursor compounds and gases for generating ultrasmall sized nanoparticles.[218] Reduction in agglomeration and narrow particle size distribution are major advantages of these pyrolysis routes. Iron oxide nanoparticles with a uniform size distribution obtained via the laser pyrolysis technique have gained considerable importance as MRI contrast agents.[234]

One of the most important applications of magnetic nanoparticles lies in the field of bimodal imaging.[235] Among the MRI contrast agents, the more common ones include paramagnetic Gd^{3+}-based complexes,[236,237] which are generally associated with problem such as rapid accumulation in the liver, thereby limiting the efficiency of these species toward imaging of specifically targeted tissues/organs. However, functionalized magnetic nanoparticles coated with a hydrophobic layer are actively involved in longer circulation time and assist in the generation of enhanced images in MRI by shortening the T_2 (transverse/spin–spin relaxation time) of water protons in the absorbing tissues.[238,239] Similarly, the lack of specificity toward the preferential targeting and killing of cancer cells has drawn considerable attention on the steps to improve the conventional cancer therapeutic models that are otherwise affecting the normal cells as well. Several reports have suggested the high temperature sensitivity of the cancer cells as compared to their normal analogues, which can be incorporated as a strategy for cancer remediation.[240] Hyperthermia-based heat treatment of cancer cells includes the utilization of superparamagnetic nanoparticles absorbing energy from an oscillating magnetic field and converting them into desired heat energy.[241] Additionally, several targeted cell gene therapy strategies have been reported to be carried out in the presence of multifunctional vectorized magnetic nanoparticles cultured in a cell monolayer and applied during in vitro magnetofection.[242] Other applications of nanoparticles involves (but not limited to) catalytic and photocatalytic degradation of organic contaminants,[243] mimicking enzymatic activities in the biosystems[244] and semiconductor based applications in light harvesting techniques and photovoltaics,[245,246] etc.

4.2.2. Encapsulation of Nanoparticles by Ferritin.

Obtaining a desired size of nanoparticles for carrying out a specific function is highly essential for any kind of application. The iron storage protein, named ferritin, is a possible solution to the majority of the problems discussed above since it can help in restricting the shape and size of nanoparticles when it is synthesized inside the nanocage.[26,27,37] Ferritin has been used in the recent past as a nanoreactor for the synthesis of a wide variety of nanoparticles by uptake of metal ions through the hydrophilic pores/channels similar to the uptake of Fe^{2+} followed by the reduction of metal precursor salts by a suitable reductant. On the other hand, preformed nanoparticles have also been successfully incorporated inside the protein nanocage by the pH/denaturant (GdnHCl or urea) dependent unfolding and folding of ferritins. Such encapsulation improves the stability, solubility, activity of those nanoparticles along with opening up the possibility of bioconjugating to a large number of biomolecules via ferritin's external/internal surface modification. The toxicity of such nanoparticles has been greatly reduced since the protein coating prevents the interaction of these nanoparticles with biological tissues and

membranes. Moreover, the protein encapsulation enhances the solubility of nanoparticles apart from preventing the unwanted leaching of the toxic ions into the physiological system. Therefore, the combination of nanoscience and bioscience can be exploited for major potential applications that could prove to be beneficial during the long run.

4.2.2.1. Via Nanoreactor Route. As described above, inorganic nanoparticles are highly promising candidates in the field of clinical applications but their interactions with the biological system proves to be harmful and toxic for biological membranes and proteins.[247,248] The toxicity originates from the reactive oxygen species (ROS) (such as superoxide, hydroxyl radicals, hydrogen peroxide) generated by the interactions of nanoparticles with the biological system leading to oxidative damage of the cells.[249,250]

Among various inorganic nanomaterials, platinum (Pt) nanoparticles have been found to mimic the activities of the biological enzymes such as catalase and superoxide dismutase in catalyzing the disproportionation reaction of hydrogen peroxide and superoxide, respectively.[251] However, Pt nanoparticles also serve as a source of toxicity owing to their ability to interact and alter the integrity and activity of biomolecules/membranes. Therefore, in order to reduce the negative impact of Pt nanoparticles, efforts have been made to deliver these nanoparticles by encapsulating them inside ferritin nanocages *via* utilization of ferritin as a nanoreactor to synthesize Pt nanoparticles inside them.[252] Zhang et al. have successfully synthesized platinum nanoparticles inside the ferritin cavity by incubating horse spleen apoferritin with K_2PtCl_4 salt and then removing the excess of salt using a desalt spin column which was followed by the chemical reduction of Pt(II) precursor to Pt(0) using $NaBH_4$.[252] The synthesized Pt nanoparticles encapsulated by apoferritin shell have been characterized by TEM images, which indicated the formation of around 2 nm sized particles inside the intact protein shell and by X-ray photoelectron spectroscopy (XPS) spectra, where the Pt 4f region appeared to be unaffected by the protein encapsulation. The ROS scavenging activity of Pt-apo ferritin nanoparticles were investigated on human intestinal carcinoma cell lines and they were found to increase cell viability by reducing the amount of hydrogen peroxide inside those cells. In addition to that, these encapsulated nanoparticles displayed long-term stability for around 2 weeks under water storage at 4 °C. Thus, ferritin here not only served as a nanoreactor synthesizing stable nanoparticles but also acted as an external surface coating agent, which prevented the harmful interaction of nanoparticle with other biological systems without inhibiting the ROS quenching abilities of the Pt nanoparticles.[252] Furthermore, Fan et al. have demonstrated the biomimetic properties of such Pt-apoferritin nanoparticles, exhibiting catalase and peroxidase activities,[84] which can be exploited as nontoxic biocatalysts against ROS induced oxidative stress (Figure.8).

Klem et al. have employed a photochemical reduction technique to successfully mineralize size constrained oxyhydroxide nanoparticles of Eu, Ti, and Fe inside the ferritin nanocages.[253] Irradiation of the xenon arc lamp on the higher oxidation state metal citrate salts resulted in the reduced state metal ions, which underwent further oxidation in the presence of oxygen forming metal oxyhydroxide nanoparticles inside the protein cages. TEM and dynamic light scattering (DLS) studies confirmed the unchanged size of the nanocomposite and intact nature of the protein shell after the mineralization
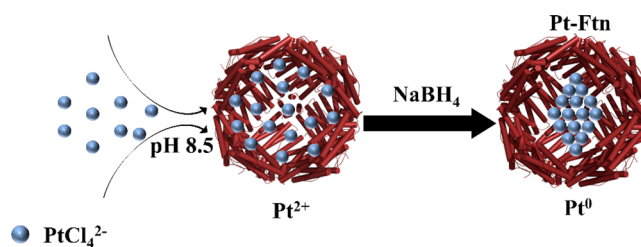
Figure 8. Schematic representation for the synthesis of Pt NPs inside ferritin protein nanocages *via* the nanoreactor route.

process. Similarly, Moglia et al. and Douglas et al. have been able to produce highly monodispersed nanoparticles by synthesizing Ag NPs and Co(O)OH NPs inside the ferritin protein *via* the nanoreactor route, respectively.[254,255] Thus, ferritin nanocages not only provided a template for the size selective synthesis of nanoparticles but also prevented the aggregation and bulk precipitation of nanoparticles. Recently, Wang et al. have successfully utilized ferritin nanocage as a nanoreactor for synthesizing ∼8 nm sized CuS nanoparticles having excellent biocompatibility and strong absorption in NIR regions required for anticancer applications.[256] Effective mitigation and treatment of tumor cells have been verified by injecting CuS-ferritin nanocomposites into U87 MG tumor bearing mice. Cancer diagnosis/treatment by hyperthermia, tumor chemo-photothermal combined therapy, MRI, and fluorescence-based targeting/imaging of tumor cells etc. have also been investigated using nanoparticles such as Fe_3O_4,[257] Co doped Fe_3O_4,[258] Prussian blue,[259] Cu,[260] $EuPO_4$ and $LuPO_4$,[261] gallic acid,[262] curcumin,[262] Au-Ag alloy,[263] etc. synthesized within the hollow internal nanocavity of ferritin protein nanocages. However, the major limitation of the nanoreactor route is associated with the narrow size (∼3−4 Å) of the ferritin pores/channels,[27,39,110,264] which might impede or restrict the diffusion/inflow of precursor salts/molecules/ions into the central nanocavity required for the generation of nanoparticles.

4.2.2.2. Via Disassembly/Reassembly Route. As discussed earlier, another alternative approach of synthesizing ferritin-encapsulated nanomaterial, which can possibly overcome the limitation associated with the nanoreactor route, involves the reversible disassembly and reassembly of ferritin protein nanocages to incorporate the nanomaterials inside them.[27,37,265] Exploiting the inherent self-assembly behavior of ferritin protein helps to engineer these multimeric nanocage architectures for facilitating the encapsulation of nanomaterials apart from overcoming limitations in terms of toxicity, solubility, biocompatibility, etc. Therefore, understanding the phenomena of ferritin self-assembly and finding the conserved interaction among its subunits holds vital importance in terms of optimization and enhancement of loading of nanomaterials and drugs inside ferritin.[37,265]

Photodynamic therapy (PDT) used for cancer treatment is largely dependent on three factor, namely, oxygen concentration, light source (≥650 nm), and a photosensitizer.[266,267] Visible light generally excites a photosensitizer molecule into a higher energy state, and this energy of the excited state is transferred to molecular oxygen leading to formation of singlet oxygen species/•OH, which display a cytotoxic effect on cancer cells inhibiting their growth. Methylene blue (MB) is one such highly efficient photosensitizer owing to its reduced toxicity and greater quantum yield in the production of singlet oxygen

species.[268] However, MB is rapidly reduced to leuko-methylene blue (LMB) by NADH/NAD(P)H inside the biological systems inactivating its photodynamic activity.[269] Therefore, in order to successfully utilize MB as a photosensitizer, Yan et al. have encapsulated MB inside equine spleen apoferritin shells by disassembling the protein nanocages at pH 2.0 and then reassembled it around MB at pH 7.5.[270] MB molecules are retained within the nanocages owing to their size (nearly 1 nm) being larger than the size of the ferritin channels (∼3−4 Å). TEM images indicated that the protein shell remained intact while fluorescence measurements revealed the presence of MB molecules inside the nanocages. The long-term stability of ferritin encapsulated MB nanocomposites was confirmed by the unchanged fluorescence intensity even after 3 weeks. The uptake of MB containing apoferritin by MCF-7 human breast cancer cells was observed to be rapid and was confirmed by confocal microscopic studies. He-Ne diode laser irradiation resulted in the generation of singlet oxygen species from apoferritin-MB nanocomposite inhibiting the growth and subsequently resulting in the death of human breast cancer cells.[270] Similarly, Liu et al. have exploited the self-assembly phenomena of ferritin to encapsulate CeO_2 nanoparticles (Figure.9) and introduced it
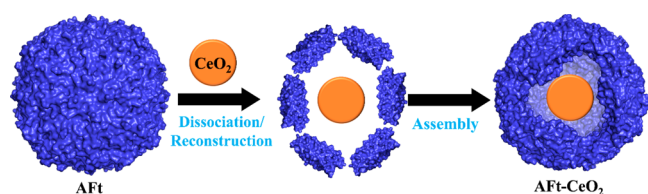
Figure 9. Schematic representation for encapsulating CeO_2 nanoparticles within apoferritin shell *via* pH dependent unfolding/refolding route.

into the human liver carcinoma cells HepG2.[271] These biocompatible AFt-CeO_2 nanoparticles behaved as an artificial redox enzyme system exhibiting excellent ROS-scavenging ability, mimicking SOD, in addition to its high cellular internalization and reduced cytotoxicity.[271]

4.2.3. Applications of Ferritin Encapsulated Nanoparticles.
4.2.3.1. Targeted Drug Delivery. The use of platinum anticancer drugs such as cisplatin, oxaliplatin, and carboplatin has been a cause of major concern based on its harmful interaction with the biological tissues leading to several kinds of toxicities such as ototoxicity, neurotoxicity, etc., and the inadequate cellular uptake of these drugs leads to the development of drug resistant tumor cells.[272] Poor water solubility and the inability to reach target sites are additional disadvantages associated with the use of these drugs.[273] A possible solution to this problem was explored by Xing et al. where the delivery of Pt-based anticancer drugs to the target site was achieved by encapsulation of these drugs inside ferritin nanocages followed by the endocytosis of the resultant apoferritin-drug complex inside the cancer cells which was achieved by the overexpression of ferritin receptors on the surface of those cells.[274] The encapsulation procedure was very similar to the one discussed above where, apoferritin was added individually to the saturated solutions of each of the above-mentioned anticancer drugs followed by dissociation of the nanocage at pH 2.0 and subsequent reassembly at pH 7.4, while the removal of drug molecules which remained outside the protein shell after the pH dependent folding-unfolding

process of ferritin was carried out using dialysis. UV−vis absorption spectra at 280 nm were comparable for AFt and AFt-drug complexes while circular dichroism (CD) spectra confirmed the unchanged secondary structure and properties of apoferritin after incorporating drug molecules. Inductively coupled plasma-mass spectrometry (ICP-MS) results suggested higher but different loading capacity for the distinct Pt-based drugs. Cytotoxicity of these apoferritin-drug complexes were tested against rat cancer cells, which overexpressed ferritin receptors facilitating the targeted drug delivery at specific sites and the results indicated greater uptake of anticancer drugs by cancer cells due to reduction in the drug resistant capacity of the tumor cells.[274] Nanoparticles and drug molecules encapsulated by ferritin have been successfully bioconjugated to iron transfer protein, transferrin, as well as to folic acid which is recognized by most of the cancer cell.[275,276] The overexpression of folate receptors on the surface of cancer cells has facilitated the receptor mediated endocytosis of the ferritin encapsulated nanoparticles/drug molecules leading to the delivery of drug molecules at the specific targeted site.[45,277]

4.2.3.2. MRI Contrast Agents. Magnetic resonance imaging (MRI) is a universal technique used in radiology for imaging the physiological processes and for detecting the micro-structures inside the body.[278] Several compounds such as gadolinium (Gd^III) chelates, superparamagnetic iron oxide nanoparticles, etc. are used as MRI contrast agents based on their magnetic properties, but their toxicity remains an issue of serious concern.[279,280] Ultrasmall superparamagnetic iron oxide nanoparticles are promising MRI contrast agents for the detection of macrophages in plaques which can cause coronary artery diseases, but the uptake of these contrast agents by macrophages have been found to be low.[281,282] Uchida et al. have mineralized iron oxide nanoparticles inside recombinant human H chain ferritin using ammonium iron(II) sulfate hexahydrate as the iron precursor and hydrogen peroxide as the oxidant.[257] The resultant mineralized protein cages exhibited enhanced macrophage uptake, stronger T_2^* (transverse relaxation) contrast, and higher relaxivity. Ferritin nanocage helped in controlling the size of iron oxide nanoparticles apart from providing an additional advantage in the form of surface modification, which is highly useful for cell-specific targeted imaging.[257] Similarly, Cai et al. have achieved active targeting and long-term imaging by utilizing the ferritins with ultrasmall maghemite/hematite cores, as a successful replacement for Gd-based T_1 contrasting agents.[283] Ferritin itself has been proposed as a natural contrast agent, and Charlton et al. have investigated the potential toxicity of horse spleen ferritin (HSF) used as an MRI contrast agent in adult male mice.[284] Neither any damaging effects nor any differences in the weight of organs were observed in cases of animals injected with HSF at doses detectable by MRI. Aime et al. have used ferritin nanocages for encapsulating Gd^III-chelates, which have resulted in reduced toxicity and higher relaxivity of the specified MRI contrast agent.[285]

4.2.3.3. Nanoelectronics. Biomineralization phenomena in the case of ferritins are a highly useful technique for protein serving as a template for the formation of inorganic materials in the core and have been utilized as a nanoblock for fabrication of nanostructures.[43,286] The process, more popularly known as the Bio-Nano process, involves the synthesis of inorganic nanocomposites within the biological protein nanocage.[286] Yamashita et al. have synthesized several metals, metal oxides, and metal hydroxide nanoparticles such as Fe_3O_4, Co_3O_4,

$Ni(OH)_2$, etc. inside the horse spleen apoferritin cavity, which holds potential usage in the field of nanodevices.[287−289] Semiconductor nanoparticles, referred to as quantum dots (QDs), have also been synthesized and/or encapsulated by an apoferritin shell, and several of its applications have been discussed in the quantum dots section of this review article. The surface negative charge of ferritin containing different nanoparticles in the form of its mineral core was utilized to selectively place a single ferritin on the surface of the silicon substrate using a nanosized disk of 3-aminopropyl-triethoxysilane (APTES) on the Si surface.[288] The protein shell was later selectively removed leading to the deposition of the nanoparticle core on the desired location on the Si surface leading to nanofabrication.

Functionalization at ferritin surface by modification of surface amino acids improves the binding efficiency of ferritin to other inorganic materials as well as to proteins. Larger two-dimensional crystals of ferritin with In_2O_3 cores based on protein−protein interactions were successfully adsorbed and nucleated on the surface of the Si substrate.[290] Heat or UV treatment have been utilized for the selective removal of titanium binding ferritin protein shell which have led to the formation and deposition of hexagonal closed packed arrays of Ti nanoparticles which are employed in nanoelectronic devices.[291,292] Growth of carbon nanotubes, metal induced lateral crystallization, and fabrication of the Si nanodisk was carried out using similar technique of selective adsorption of ferritin containing metal nanoparticles core on the surface of the substrate followed by removal of the protein shell leading to deposition of metal nanoparticle on the substrate.[293,294] Use of highly pure protein, controlled adsorption, and selective placement of protein on the surface of the substrate holds the key in the design of highly efficient nanodevices for nanoelectronics and catalytic purposes[288] (Figure.10).
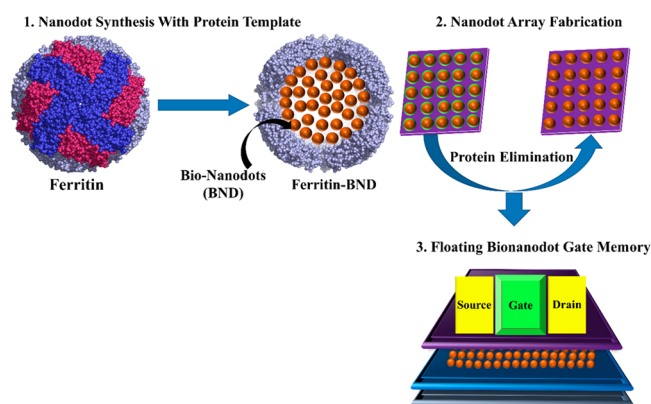
Figure 10. Schematic representation for synthesis and nanoelectronic applications of ferritin encapsulated Co_3O_4 nanoparticles.

Furthermore, Colton et al. and Smith et al. have investigated the ability to synthesize non-naturally occurring minerals inside ferritin (by co-deposition of iron with different oxo-anions), which generates a wide range of possibilities to design a library of ferritin containing nanoparticles with altered as well as tunable band gaps for their utilization in multijunction photovoltaic applications.[295,296] Such alterations in mineral structure could also prove to be useful to potentially exploit the ferritin protein nanocages with novel iron-oxo-anion based mixed mineral structures having differences in their size,

structure, color, crystallinity/morphology, optical, magnetic, electronic properties, etc. for light harvesting and photo-catalytic applications.[295,296]

4.2.3.4. Catalysis and Photocatalysis. Ferritin has been successfully employed as a template/scaffold for the synthesis of a large number of nanoparticles in the recent past accounting for its role as a nanoreactor.[43,286] Pd, Ir, and Rh nanoparticles synthesized within the ferritin protein shell exhibited enhanced catalytic activity toward the catalytic discoloration of congo red dye,[297] as investigated by Pekarik et al. Similarly, Kumari et al. and Peskova et al. have also reported such improvement in catalytic efficiency toward the degradation of azo dyes as observed in the case of Au, Ag, and Pd nanoparticles upon encapsulation by ferritin biotem-plate.[298,299]

Apart from its role as a nanoreactor, an interesting result have been reported by Keyes et al. where the ferrihydrite mineral core of ferritin acted as a photocatalyst for the synthesis of gold nanoparticles.[300] In general, the photo-chemical synthesis of gold nanoparticles can serve as an alternative to the conventional synthetic strategies involving the reduction of gold salts using harmful chemicals and reducing agents. Generation of an electron−hole pair in the ferrihydrite mineral core upon light irradiation is believed to be the driving force in the photochemical reduction of gold precursor salt based on its interaction with electron donors and acceptors. The synthesis was carried out in the presence of a Hg lamp, ferritin solution, electron donor citrate, and gold chloride salt. Experiments were also performed in the absence of citrate where 3-(N-morpholino)propanesulfonic acid (MOPS) buffer emerged as an alternative to citrate as an electron donor. The proposed mechanism suggested the entry of Au^{3+} ions into the protein nanocages through the channels on the surface of ferritin while the mineral core acted as the nucleation site for the photochemical reduction of Au(III) to Au(0).[300] The mineral core upon expose to light produced an electron to reduce the gold salt while the hole generated was refilled by the electron donor citrate/MOPS buffer. UV−vis spectra demonstrated the formation of Au nanoparticles by the appearance of a characteristic surface plasmon resonance peak at 530 nm while TEM images indicated the formation of ∼6 nm sized particles. The formation of Au nanoparticles inside the ferritin cavity was further confirmed by size exclusion chromatography (SEC), where the eluted sample displayed strong peaks at 530 nm (for Au nanoparticles) and at 280 nm (for protein). A metal nucleation site was even reported at the external surface of ferritin due to presence of "gold binding" cysteine residues located at 3-fold channels which accounts for the formation of Au nanoparticles at the exterior surface of ferritin. The formation of gold nanoparticles both on the external and internal surfaces of ferritin was reported, and the proposed mechanism can serve as a model system for the delivery of Au nanoparticles into the biological systems.[300] A similar mechanism of photocatalytic activity of horse spleen ferritin has been reported by Saenz et al. where the excited electron of the core produced upon light irradiation reduces the mineral core itself releasing Fe^{2+} ions which either reduces any electron acceptor or is grabbed by any chelator, if present.[301]

5. CONCLUSIONS AND PERSPECTIVES

The current review highlights recent developments toward the accumulation of different metal ions inside the ferritin cage for

Table 3. Synthetic Routes and Applications of Ferritin Encapsulated Nanoparticles

ferritin type	mineral core	core size (nm)[a]	synthetic route	applications and proposed applications	refs
horse spleen ferritin	Pt	2	nanoreactor (reduction)	antioxidant against ROS-mediated diseases	252
mammalian ferritin	Eu(O)OH, Ti(O)OH, Fe(O)OH	5.7 ± 1	nanoreactor (photochemical reduction)	size-constrained synthesis of unattainable oxyhydroxide nanomaterials	253
recombinant rat ferritin	CuS	8	nanoreactor	cancer theranostics	256
recombinant human H ferritin	Fe_3O_4	3.6−5.9	nanoreactor	MRI contrast agents	257
PEGylated recombinant human H ferritin	Co doped Fe_3O_4	6.0−6.8	nanoreactor	hyperthermia treatment for melanoma	258
mammalian ferritin	CeO_2	4.5	pH-based disassembly/reassembly	artificial redox enzyme mimicking SOD activity.	271
recombinant human H ferritin	α-Fe_2O_3 (or) γ-Fe_2O_3	1.6−4.7	nanoreactor	MRI contrast agents	283
horse spleen ferritin	Pt	1.9 ± 0.4	nanoreactor (reduction)	enzymatic (catalase and peroxidase) activities	84
horse spleen ferritin	ferrihydrite $nFe_2O_3 \cdot xH_2O$		native (commercially purchased)	MRI contrast agents	284
E. coli Dps mini ferritin	Au		nanoreactor	high throughput screening of protein libraries	302
equine spleen ferritin	ferrihydrite ($Fe_2O_3 \cdot xH_2O$)	6−8	nanoreactor	tunable band gap for semiconductor-based applications	295
equine spleen ferritin	Au	3.8 ± 0.1	nanoreactor	catalytic activity during nitro reduction reactions	298
horse spleen ferritin	Prussian blue $Fe_4[Fe(CN)_6]_3$		nanoreactor	photothermal cancer therapy	259
recombinant human H ferritin	Fe_3O_4	4.7	nanoreactor	targeting and visualizing tumor cells	83
recombinant human H and L ferritin	Ag	5.3−5.4	nanoreactor (reduction)	size constrained nanomaterial synthesis for biomedical applications	254
horse spleen ferritin	Co(O)OH	7.0	nanoreactor	size constrained nanomaterial synthesis	255
recombinant human ferritin	Cu		nanoreactor	improving the therapeutic efficacy of disulfiram in tumor therapy	260
recombinant Pyrococcus furiosus ferritin	Pd, Rh, Ir		nanoreactor	catalytic degradation of azo dyes	297
horse spleen ferritin	Co		nanoreactor	electrochemical biosensor to determine ascorbic acid	303
recombinant human H ferritin	Fe_3O_4 (or) γ-Fe_2O_3	3.8−6.0	nanoreactor	targeting of cancer cells	82
horse spleen ferritin	ferrihydrite doped with halides/oxo-anions	8.3−9.1	nanoreactor	light harvesting and photocatalytic applications	296
recombinant human H ferritin	Cu		nanoreactor	enhancing the pharmacological effect of ascorbate in cancer therapy	304
horse spleen ferritin	$EuPO_4$, $LuPO_4$	8.0	nanoreactor	simultaneous determination of two phosphorylated p53 proteins in SCC-7 cells for early diagnosis of cancer	261
recombinant human mitochondrial ferritin	Au	<2	nanoreactor	potentially exploited for the generation of a variety of fluorescent hybrid nanomaterials	305
recombinant human H ferritin	gallic acid, curcumin	7.3 ± 0.2	pH-based disassembly/reassembly	fabricating nanomaterials in the emerging field of nanomedicine and tumor imaging	262
recombinant human H ferritin	$Co_xFe_{3-x}O_4$	5.4−5.8	nanoreactor	enhanced peroxidase activity and tumor tissue visualization	306
horse spleen ferritin	Au-Ag alloy		nanoreactor	cryoprotection against ROS induced oxidative stress	263
recombinant Pyrococcus furiosus ferritin	Ag, Pd	4.2−4.7	nanoreactor	catalytic activity toward reduction of azo dyes	299
equine spleen ferritin	methylene blue		pH-based disassembly/reassembly	targeted imaging and cancer therapy	270
recombinant horse spleen ferritin	In_2O_3	6.6 ± 0.5	nanoreactor	semiconductor based applications in electronic devices	307

[a]Determined from TEM analysis.

the synthesis of nanomaterials for biomedical applications. Understanding the metal-protein interactions and their translocation/binding mechanisms would assist in the synthesis of novel bionanomaterials. Construction of new functionalized bionanomaterials can be performed by creating new metal ion binding sites *via* site-specific mutagenesis, thereby utilizing ferritin cage as a template/nanosink. Song et al. have recently

highlighted the importance of various cargo-loaded human ferritins for biomedical applications and design of nanomedicine by essentially focusing on the physicochemical characteristics and intrinsic tumor-targeting properties of such ferritin-based formulations.[308]

QDs are promising materials for utilization in nanotechnology and biomedical applications based on their size

dependent tunable opto-electronic properties.[115,141] However, its severe toxicity, poor solubility, reduced quantum yield, and unwanted side reactions inside biological system restricted their usage in various biomedical applications. Encapsulation of QDs by ferritin nanocages either *via* the nanoreactor route (where intact hydrophilic pores/channels of ferritins serve as the entry route for various ions during the synthesis of nanomaterials) or *via* the disassembly/reassembly process has resolved the above-mentioned problems to a greater extent leading to their utilization in applications ranging from photovoltaics to targeted drug delivery (Table 2). Thus, ferritin nanocages have emerged as a potential nanoreactor for the synthesis of QDs and as protective coating agents for QDs to prevent the release of toxic metal ions into the biological system. It enhanced the biocompatibility of QDs as well as its solubility. Dps protein, also known as mini ferritins,[26,27,44,286] having an internal diameter of ∼5 nm, can prove to be highly useful in tuning the optical properties and enhancing the fluorescence quantum yields of QDs by the size selective synthesis/incorporation of smaller sized QDs (<5 nm). Further functionalization over the surface of ferritin encapsulated QDs can be used for various applications such as targeted delivery of QDs at the specific site, fluorescence imaging of tissue sections/bioimaging agents for tracking tumor growth, gene analysis, etc. Problems similar to QDs arise in the case of nanoparticles which also have resemblance in the usage of ferritin as a capping agent. The concept of self-assembly of ferritin can be utilized in the design of hybrid ferritin by disassembling two different kinds of ferritin and then reassembling them with the incorporation of nanoparticles inside their nanocavity.[37]

With the advent of nanotechnology in the recent past, the process of nanomaterial synthesis along with the ability to tailor their functional properties (as per targeted biomedical applications) has witnessed significant improvements.[43] However, the generation of uniform, stable, and highly monodispersed superparamagnetic nanoparticles remains a critical demand for biomedical research, and therefore, future efforts should be directed toward overcoming the challenges in the design and development of safer, biocompatible nano-medicines. Ferritin encapsulation of nanoparticles helps in eliminating major hindrances associated with the use of nanoparticles in biomedical applications such as toxicity, poor solubility, imitation of harmful side reactions with biological systems, etc. (Table 3). A better understanding of ferritin self-assembly would be highly useful for the incorporation of nanoparticles *via* the unfolding/refolding process.[27,37] The formation of hybrid ferritin containing multiple nanoparticles would also open up a wide range of possibilities for conjugation with a large number of biomolecules.[35,43,277]

■ AUTHOR INFORMATION

Corresponding Author

Rabindra K. Behera − *Department of Chemistry, National Institute of Technology, Rourkela 769008 Odisha, India;* ⊙ orcid.org/0000-0003-2849-3292; Phone: +91-661-2462980; Email: beherarabi@nitrkl.ac.in; Fax: +91-661-2462651

Authors

Abhinav Mohanty − *Department of Chemistry, National Institute of Technology, Rourkela 769008 Odisha, India;* ⊙ orcid.org/0000-0002-3843-1960

Akankshika Parida − *Department of Chemistry, National Institute of Technology, Rourkela 769008 Odisha, India;* ⊙ orcid.org/0000-0002-8483-3821

Rohit Kumar Raut − *Department of Chemistry, National Institute of Technology, Rourkela 769008 Odisha, India*

Complete contact information is available at:
https://pubs.acs.org/10.1021/acsbiomedchemau.2c00003

Notes

The authors declare no competing financial interest.

■ ABBREVIATIONS

AFt, apoferritin; Ftn, ferritin; Bfr, bacterioferritins; Dps, DNA-binding proteins from starved cells; HSF, horse spleen ferritin; F_{ox}, ferroxidase center; NPs, nanoparticles; QDs, quantum dots; SPION, superparamagnetic iron oxide nanoparticles; CD, circular dichroism; DLS, dynamic light scattering; TEM, transmission electron microscopy; PAGE, polyacrylamide gel electrophoresis; XPS, X-ray photoelectron spectroscopy; APTES, 3-aminopropyl-triethoxysilane; MOPS, 3-(*N*-morpholino)propanesulfonic acid; MRI, magnetic resonance imaging; ROS, reactive oxygen species

■ REFERENCES

(1) Chan, W. C. W. Bionanotechnology Progress and Advances. *Biology of Blood and Marrow Transplantation* **2006**, *12* (1), 87−91.

(2) Rohela, G. K.; Srinivasulu, Y.; Rathore, M. S. A Review Paper on Recent Trends in Bio-nanotechnology: Implications and Potentials. *Nanoscience & Nanotechnology-Asia* **2018**, *9* (1), 12−20.

(3) Englebienne, P.; Hoonacker, A. V. Bionanotechnology: The Science of Revealing Life with Nanostructures. *Current Nanoscience* **2005**, *1* (2), 97−106.

(4) Jain, K. K. The role of nanobiotechnology in drug discovery. *Drug Discovery Today* **2005**, *10* (21), 1435−1442.

(5) Khan, I.; Khan, M.; Umar, M. N.; Oh, D. H. Nanobiotechnology and its applications in drug delivery system: a review. *IET Nanobiotechnol* **2015**, *9* (6), 396−400.

(6) Vareda, J. P.; Valente, A. J. M.; Durães, L. Assessment of heavy metal pollution from anthropogenic activities and remediation strategies: A review. *Journal of Environmental Management* **2019**, *246*, 101−118.

(7) Tchounwou, P. B.; Yedjou, C. G.; Patlolla, A. K.; Sutton, D. J. Heavy metal toxicity and the environment. *Exp Suppl* **2012**, *101*, 133−164.

(8) Mishra, S.; Bharagava, R. N.; More, N.; Yadav, A.; Zainith, S.; Mani, S.; Chowdhary, P. Heavy Metal Contamination: An Alarming Threat to Environment and Human Health. In *Environmental Biotechnology: For Sustainable Future*; Springer: Singapore, 2019; p 103,.

(9) Vardhan, K. H.; Kumar, P. S.; Panda, R. C. A review on heavy metal pollution, toxicity and remedial measures: Current trends and future perspectives. *J. Mol. Liq.* **2019**, *290*, 111197.

(10) Sears, M. E. Chelation: Harnessing and Enhancing Heavy Metal Detoxification—A Review. *The Scientific World Journal* **2013**, *2013*, 219840.

(11) Kim, J.-J.; Kim, Y.-S.; Kumar, V. Heavy metal toxicity: An update of chelating therapeutic strategies. *Journal of Trace Elements in Medicine and Biology* **2019**, *54*, 226−231.

(12) Koedrith, P.; Kim, H.; Weon, J.-I.; Seo, Y. R. Toxicogenomic approaches for understanding molecular mechanisms of heavy metal mutagenicity and carcinogenicity. *International Journal of Hygiene and Environmental Health* **2013**, *216* (5), 587−598.

(13) Zeraatkar, A. K.; Ahmadzadeh, H.; Talebi, A. F.; Moheimani, N. R.; McHenry, M. P. Potential use of algae for heavy metal bioremediation, a critical review. *Journal of Environmental Management* **2016**, *181*, 817−831.

(14) Zhang, Y.; Li, M.; Gao, X.; Chen, Y.; Liu, T. Nanotechnology in cancer diagnosis: progress, challenges and opportunities. *J. Hematol. Oncol.* **2019**, *12*, 137.

(15) Zugazagoitia, J.; Guedes, C.; Ponce, S.; Ferrer, I.; Molina-Pinelo, S.; Paz-Ares, L. Current Challenges in Cancer Treatment. *Clinical Therapeutics* **2016**, *38* (7), 1551−1566.

(16) Guan, X. Cancer metastases: challenges and opportunities. *Acta Pharmaceutica Sinica B* **2015**, *5* (5), 402−418.

(17) Sajid, M.; Ilyas, M.; Basheer, C.; Tariq, M.; Daud, M.; Baig, N.; Shehzad, F. Impact of nanoparticles on human and environment: review of toxicity factors, exposures, control strategies, and future prospects. *Environmental Science and Pollution Research* **2015**, *22* (6), 4122−4143.

(18) Srivastava, V.; Gusain, D.; Sharma, Y. C. Critical Review on the Toxicity of Some Widely Used Engineered Nanoparticles. *Ind. Eng. Chem. Res.* **2015**, *54* (24), 6209−6233.

(19) Jeevanandam, J.; Barhoum, A.; Chan, Y. S.; Dufresne, A.; Danquah, M. K. Review on nanoparticles and nanostructured materials: history, sources, toxicity and regulations. *Beilstein J Nanotechnol* **2018**, *9*, 1050−1074.

(20) Spicer, C. D.; Jumeaux, C.; Gupta, B.; Stevens, M. M. Peptide and protein nanoparticle conjugates: versatile platforms for biomedical applications. *Chemical Society Reviews* **2018**, *47* (10), 3574−3620.

(21) Rana, S.; Yeh, Y.-C.; Rotello, V. M. Engineering the nanoparticle−protein interface: applications and possibilities. *Current Opinion in Chemical Biology* **2010**, *14* (6), 828−834.

(22) Zan, G.; Wu, Q. Biomimetic and Bioinspired Synthesis of Nanomaterials/Nanostructures. *Adv. Mater.* **2016**, *28* (11), 2099−2147.

(23) Chiu, C.-Y.; Ruan, L.; Huang, Y. Biomolecular specificity controlled nanomaterial synthesis. *Chemical Society Reviews* **2013**, *42* (7), 2512−2527.

(24) Chen, Y.; Feng, Y.; Deveaux, J. G.; Masoud, M. A.; Chandra, F. S.; Chen, H.; Zhang, D.; Feng, L. Biomineralization Forming Process and Bio-inspired Nanomaterials for Biomedical Application: A Review. *Minerals* **2019**, *9* (2), 68.

(25) Theil, E. C. Ferritin: The Protein Nanocage and Iron Biomineral in Health and in Disease. *Inorg. Chem.* **2013**, *52* (21), 12223.

(26) Theil, E. C.; Tosha, T.; Behera, R. K. Solving Biology's Iron Chemistry Problem with Ferritin Protein Nanocages. *Acc. Chem. Res.* **2016**, *49* (5), 784−91.

(27) Theil, E. C.; Behera, R. K.; Tosha, T. Ferritins for chemistry and for life. *Coord. Chem. Rev.* **2013**, *257*, 579−586.

(28) Theil, E. C. Ferritin: structure, gene regulation, and cellular function in animals, plants, and microorganisms. *Annual review of biochemistry* **1987**, *56*, 289−315.

(29) Koochana, P. K.; Mohanty, A.; Das, S.; Subhadarshanee, B.; Satpati, S.; Dixit, A.; Sabat, S. C.; Behera, R. K. Releasing iron from ferritin protein nanocage by reductive method: The role of electron transfer mediator. *Biochim Biophys Acta Gen Subj* **2018**, *1862* (5), 1190−1198.

(30) Koochana, P. K.; Mohanty, A.; Subhadarshanee, B.; Satpati, S.; Naskar, R.; Dixit, A.; Behera, R. K. Phenothiazines and phenoxazines:

as electron transfer mediators for ferritin iron release. *Dalton Trans* **2019**, *48* (10), 3314−3326.

(31) Koochana, P. K.; Mohanty, A.; Parida, A.; Behera, N.; Behera, P. M.; Dixit, A.; Behera, R. K. Flavin-mediated reductive iron mobilization from frog M and Mycobacterial ferritins: impact of their size, charge and reactivities with NADH/O2. *J Biol Inorg Chem* **2021**, *26* (2−3), 265−281.

(32) Cassat, J. E.; Skaar, E. P. Iron in Infection and Immunity. *Cell Host Microbe* **2013**, *13* (5), 509−519.

(33) Hu, Y.; Li, F.; Liu, C.; Rosso, K.; Shi, Z. Iron Redox Chemistry and Its Environmental Impact: A Virtual Special Issue. *ACS Earth and Space Chemistry* **2019**, *3* (11), 2374−2375.

(34) Mohanty, A.; Subhadarshanee, B.; Barman, P.; Mahapatra, C.; Aishwarya, B.; Behera, R. K. Iron Mineralizing Bacterioferritin A from Mycobacterium tuberculosis Exhibits Unique Catalase-Dps-like Dual Activities. *Inorganic chemistry* **2019**, *58* (8), 4741−4752.

(35) Subhadarshanee, B.; Mohanty, A.; Jagdev, M. K.; Vasudevan, D.; Behera, R. K. Surface charge dependent separation of modified and hybrid ferritin in native PAGE: Impact of lysine 104. *Biochim Biophys Acta Proteins Proteom* **2017**, *1865* (10), 1267−1273.

(36) Parida, A.; Mohanty, A.; Kansara, B. T.; Behera, R. K. Impact of Phosphate on Iron Mineralization and Mobilization in Nonheme Bacterioferritin B from Mycobacterium tuberculosis. *Inorg Chem* **2020**, *59* (1), 629−641.

(37) Mohanty, A.; K, M.; Jena, S. S.; Behera, R. K. Kinetics of Ferritin Self-Assembly by Laser Light Scattering: Impact of Subunit Concentration, pH, and Ionic Strength. *Biomacromolecules* **2021**, *22* (4), 1389−1398.

(38) Mohanty, A.; Parida, A.; Subhadarshanee, B.; Behera, N.; Subudhi, T.; Koochana, P. K.; Behera, R. K. Alteration of Coaxial Heme Ligands Reveals the Role of Heme in Bacterioferritin from Mycobacterium tuberculosis. *Inorganic chemistry* **2021**, *60* (22), 16937−16952.

(39) Behera, R. K.; Theil, E. C. Moving Fe2+ from ferritin ion channels to catalytic OH centers depends on conserved protein cage carboxylates. *Proceedings of the National Academy of Sciences of the United States of America* **2014**, *111* (22), 7925−7930.

(40) Behera, R. K.; Torres, R.; Tosha, T.; Bradley, J. M.; Goulding, C. W.; Theil, E. C. Fe(2+) substrate transport through ferritin protein cage ion channels influences enzyme activity and biomineralization. *J Biol Inorg Chem* **2015**, *20* (6), 957−969.

(41) Bou-Abdallah, F. The iron redox and hydrolysis chemistry of the ferritins. *Biochimica et Biophysica Acta (BBA) - General Subjects* **2010**, *1800* (8), 719−731.

(42) Dehner, C.; Morales-Soto, N.; Behera, R. K.; Shrout, J.; Theil, E. C.; Maurice, P. A.; Dubois, J. L. Ferritin and ferrihydrite nanoparticles as iron sources for Pseudomonas aeruginosa. *J Biol Inorg Chem* **2013**, *18* (3), 371−81.

(43) Jutz, G.; van Rijn, P.; Santos Miranda, B.; Boeker, A. Ferritin: A Versatile Building Block for Bionanotechnology. *Chem. Rev. (Washington, DC, U. S.)* **2015**, *115*, 1653−1701.

(44) Honarmand Ebrahimi, K.; Hagedoorn, P.-L.; Hagen, W. R. Unity in the Biochemistry of the Iron-Storage Proteins Ferritin and Bacterioferritin. *Chemical Reviews* **2015**, *115* (1), 295−326.

(45) Tesarova, B.; Musilek, K.; Rex, S.; Heger, Z. Taking advantage of cellular uptake of ferritin nanocages for targeted drug delivery. *J. Controlled Release* **2020**, *325*, 176−190.

(46) Schwartz, J. K.; Liu, X. S.; Tosha, T.; Theil, E. C.; Solomon, E. I. Spectroscopic definition of the ferroxidase site in M ferritin: comparison of binuclear substrate vs cofactor active sites. *J. Am. Chem. Soc.* **2008**, *130* (29), 9441−50.

(47) Tosha, T.; Ng, H. L.; Bhattasali, O.; Alber, T.; Theil, E. C. Moving metal ions through ferritin-protein nanocages from three-fold pores to catalytic sites. *J. Am. Chem. Soc.* **2010**, *132* (41), 14562−14569.

(48) Bradley, J. M.; Moore, G. R.; Le Brun, N. E. Mechanisms of iron mineralization in ferritins: one size does not fit all. *JBIC Journal of Biological Inorganic Chemistry* **2014**, *19* (6), 775−785.

(49) Bradley, J. M.; Moore, G. R.; Le Brun, N. E. Diversity of Fe2+ entry and oxidation in ferritins. *Current Opinion in Chemical Biology* **2017**, *37*, 122−128.

(50) Bradley, J. M.; Pullin, J.; Moore, G. R.; Svistunenko, D. A.; Hemmings, A. M.; Le Brun, N. E. Routes of iron entry into, and exit from, the catalytic ferroxidase sites of the prokaryotic ferritin SynFtn. *Dalton Trans* **2020**, *49* (5), 1545−1554.

(51) Mehlenbacher, M.; Poli, M.; Arosio, P.; Santambrogio, P.; Levi, S.; Chasteen, N. D.; Bou-Abdallah, F. Iron Oxidation and Core Formation in Recombinant Heteropolymeric Human Ferritins. *Biochemistry* **2017**, *56* (30), 3900−3912.

(52) Zhao, G.; Bou-Abdallah, F.; Arosio, P.; Levi, S.; Janus-Chandler, C.; Chasteen, N. D. Multiple Pathways for Mineral Core Formation in Mammalian Apoferritin. The Role of Hydrogen Peroxide. *Biochemistry* **2003**, *42* (10), 3142−3150.

(53) Chasteen, N. D.; Harrison, P. M. Mineralization in ferritin: an efficient means of iron storage. *Journal of structural biology* **1999**, *126* (3), 182−194.

(54) Bellapadrona, G.; Stefanini, S.; Zamparelli, C.; Theil, E. C.; Chiancone, E. Iron translocation into and out of Listeria innocua Dps and size distribution of the protein-enclosed nanomineral are modulated by the electrostatic gradient at the 3-fold "ferritin-like" pores. *The Journal of biological chemistry* **2009**, *284* (28), 19101−19109.

(55) Ceci, P.; Di Cecca, G.; Falconi, M.; Oteri, F.; Zamparelli, C.; Chiancone, E. Effect of the charge distribution along the "ferritin-like" pores of the proteins from the Dps family on the iron incorporation process. *J Biol Inorg Chem* **2011**, *16* (6), 869−880.

(56) Gupta, S.; Chatterji, D. Bimodal Protection of DNA by Mycobacterium smegmatis DNA-binding Protein from Stationary Phase Cells. *J. Biol. Chem.* **2003**, *278* (7), 5235−5241.

(57) Ghatak, P.; Karmakar, K.; Kasetty, S.; Chatterji, D. Unveiling the Role of Dps in the Organization of Mycobacterial Nucleoid. *PloS one* **2011**, *6* (1), No. e16019.

(58) Wong, S. G.; Grigg, J. C.; Le Brun, N. E.; Moore, G. R.; Murphy, M. E.; Mauk, A. G. The B-type channel is a major route for iron entry into the ferroxidase center and central cavity of bacterioferritin. *J. Biol. Chem.* **2015**, *290* (6), 3732−3739.

(59) Gupta, V.; Gupta, R. K.; Khare, G.; Salunke, D. M.; Tyagi, A. K. Cloning, expression, purification, crystallization and preliminary X-ray crystallographic analysis of bacterioferritin A from Mycobacterium tuberculosis. *Acta Crystallographica Section F* **2008**, *64* (5), 398−401.

(60) Gupta, V.; Gupta, R. K.; Khare, G.; Salunke, D. M.; Tyagi, A. K. Crystal Structure of Bfr A from Mycobacterium tuberculosis: Incorporation of Selenomethionine Results in Cleavage and Demetallation of Haem. *PloS one* **2009**, *4* (11), No. e8028.

(61) Rivera, M. Bacterioferritin: Structure, Dynamics, and Protein-Protein Interactions at Play in Iron Storage and Mobilization. *Acc. Chem. Res.* **2017**, *50* (2), 331−340.

(62) Rivera, M. *Bacterioferritin: Structure Function and Protein−Protein Interactions*, 30th ed.; World Scientific Publishing Co. Pte. Ltd.: Singapore, 2013; pp 135−178.

(63) Kwak, Y.; Schwartz, J. K.; Haldar, S.; Behera, R. K.; Tosha, T.; Theil, E. C.; Solomon, E. I. Spectroscopic studies of single and double variants of M ferritin: lack of conversion of a biferrous substrate site into a cofactor site for O2 activation. *Biochemistry* **2014**, *53* (3), 473−82.

(64) Theil, E. C.; Behera, R. K. *The Chemistry of Nature's Iron Biominerals in Ferritin Protein Nanocages*; Wiley, 2012; pp 1−15.

(65) Aitken-Rogers, H.; Singleton, C.; Lewin, A.; Taylor-Gee, A.; Moore, G. R.; Le Brun, N. E. Effect of phosphate on bacterioferritin-catalysed iron(II) oxidation. *J Biol Inorg Chem* **2004**, *9* (2), 161−70.

(66) Hilton, R. J.; David Andros, N.; Watt, R. K. The ferroxidase center is essential for ferritin iron loading in the presence of phosphate and minimizes side reactions that form Fe(III)-phosphate colloids. *Biometals* **2012**, *25* (2), 259−73.

(67) Treffry, A.; Bauminger, E. R.; Hechel, D.; Hodson, N. W.; Nowik, I.; Yewdall, S. J.; Harrison, P. M. Defining the roles of the threefold channels in iron uptake, iron oxidation and iron-core

(68) Liu, X.; Theil, E. C. Ferritins: dynamic management of biological iron and oxygen chemistry. *Acc. Chem. Res.* **2005**, *38* (3), 167−75.

formation in ferritin: a study aided by site-directed mutagenesis. *The Biochemical journal* **1993**, *296* (3), 721−728.

(69) Yang, X.; Chen-Barrett, Y.; Arosio, P.; Chasteen, N. D. Reaction Paths of Iron Oxidation and Hydrolysis in Horse Spleen and Recombinant Human Ferritins. *Biochemistry* **1998**, *37* (27), 9743−9750.

(70) Kell, D. B.; Pretorius, E. Serum ferritin is an important inflammatory disease marker, as it is mainly a leakage product from damaged cells. *Metallomics: integrated biometal science* **2014**, *6* (4), 748−73.

(71) Bevers, L. E.; Theil, E. C. Maxi- and mini-ferritins: minerals and protein nanocages. *Progress in molecular and subcellular biology* **2011**, *52*, 29−47.

(72) Wade, V. J.; Levi, S.; Arosio, P.; Treffry, A.; Harrison, P. M.; Mann, S. Influence of site-directed modifications on the formation of iron cores in ferritin. *Journal of molecular biology* **1991**, *221* (4), 1443−52.

(73) Levi, S.; Yewdall, S. J.; Harrison, P. M.; Santambrogio, P.; Cozzi, A.; Rovida, E.; Albertini, A.; Arosio, P. Evidence of H- and L-chains have co-operative roles in the iron-uptake mechanism of human ferritin. *Biochem. J.* **1992**, *288* (2), 591−596.

(74) Toussaint, L.; Bertrand, L.; Hue, L.; Crichton, R. R.; Declercq, J. P. High-resolution X-ray structures of human apoferritin H-chain mutants correlated with their activity and metal-binding sites. *Journal of molecular biology* **2007**, *365* (2), 440−52.

(75) Bertini, I.; Lalli, D.; Mangani, S.; Pozzi, C.; Rosa, C.; Theil, E. C.; Turano, P. Structural insights into the ferroxidase site of ferritins from higher eukaryotes. *J. Am. Chem. Soc.* **2012**, *134* (14), 6169−6176.

(76) Maity, B.; Hishikawa, Y.; Lu, D.; Ueno, T. Recent progresses in the accumulation of metal ions into the apo-ferritin cage: Experimental and theoretical perspectives. *Polyhedron* **2019**, *172*, 104−111.

(77) Harrison, P. M. Iron storage in bacteria. *Nature* **1979**, *279* (5708), 15−6.

(78) Harrison, P. M.; Fischbach, F. A.; Hoy, T. G.; Haggis, G. H. Ferric oxyhydroxide core of ferritin. *Nature* **1967**, *216* (5121), 1188−90.

(79) Crichton, R. R.; Declercq, J. P. X-ray structures of ferritins and related proteins. *Biochimica et biophysica acta* **2010**, *1800* (8), 706−718.

(80) Maity, B.; Fujita, K.; Ueno, T. Use of the confined spaces of apo-ferritin and virus capsids as nanoreactors for catalytic reactions. *Curr Opin Chem Biol* **2015**, *25*, 88−97.

(81) Tatur, J.; Hagen, W. R.; Matias, P. M. Crystal structure of the ferritin from the hyperthermophilic archaeal anaerobe Pyrococcus furiosus. *J Biol Inorg Chem* **2007**, *12* (5), 615−30.

(82) Uchida, M.; Flenniken, M. L.; Allen, M.; Willits, D. A.; Crowley, B. E.; Brumfield, S.; Willis, A. F.; Jackiw, L.; Jutila, M.; Young, M. J.; Douglas, T. Targeting of Cancer Cells with Ferrimagnetic Ferritin Cage Nanoparticles. *J. Am. Chem. Soc.* **2006**, *128* (51), 16626−16633.

(83) Fan, K.; Cao, C.; Pan, Y.; Lu, D.; Yang, D.; Feng, J.; Song, L.; Liang, M.; Yan, X. Magnetoferritin nanoparticles for targeting and visualizing tumour tissues. *Nature Nanotechnology* **2012**, *7* (7), 459−464.

(84) Fan, J.; Yin, J.-J.; Ning, B.; Wu, X.; Hu, Y.; Ferrari, M.; Anderson, G. J.; Wei, J.; Zhao, Y.; Nie, G. Direct evidence for catalase and peroxidase activities of ferritin−platinum nanoparticles. *Bio-materials* **2011**, *32* (6), 1611−1618.

(85) Haldar, S.; Bevers, L. E.; Tosha, T.; Theil, E. C. Moving Iron through ferritin protein nanocages depends on residues throughout each four alpha-helix bundle subunit. *J. Biol. Chem.* **2011**, *286* (29), 25620−25627.

(86) Tosha, T.; Hasan, M. R.; Theil, E. C. The ferritin Fe2 site at the diiron catalytic center controls the reaction with O$_2$ in the rapid

mineralization pathway. *Proceedings of the National Academy of Sciences* **2008**, *105* (47), 18182.

(87) Bradley, J. M.; Le Brun, N. E.; Moore, G. R. Ferritins: furnishing proteins with iron. *J Biol Inorg Chem* **2016**, *21* (1), 13−28.

(88) Pozzi, C.; Di Pisa, F.; Lalli, D.; Rosa, C.; Theil, E.; Turano, P.; Mangani, S. Time-lapse anomalous X-ray diffraction shows how Fe(2+) substrate ions move through ferritin protein nanocages to oxidoreductase sites. *Acta crystallographica. Section D, Biological crystallography* **2015**, *71* (4), 941−953.

(89) Chandramouli, B.; Bernacchioni, C.; Di Maio, D.; Turano, P.; Brancato, G. Electrostatic and Structural Bases of Fe2+ Translocation through Ferritin Channels. *J. Biol. Chem.* **2016**, *291* (49), 25617−25628.

(90) Douglas, T.; Ripoll, D. R. Calculated electrostatic gradients in recombinant human H-chain ferritin. *Protein science: a publication of the Protein Society* **1998**, *7* (5), 1083−1091.

(91) Chandramouli, B.; Del Galdo, S.; Mancini, G.; Barone, V. Mechanistic insights into metal ions transit through threefold ferritin channel. *Biochim Biophys Acta Gen Subj* **2019**, *1863* (2), 472−480.

(92) Arosio, P.; Ingrassia, R.; Cavadini, P. Ferritins: a family of molecules for iron storage, antioxidation and more. *Biochimica et biophysica acta* **2009**, *1790* (7), 589−99.

(93) Rui, H.; Rivera, M.; Im, W. Protein dynamics and ion traffic in bacterioferritin. *Biochemistry* **2012**, *51* (49), 9900−10.

(94) Yao, H.; Rui, H.; Kumar, R.; Eshelman, K.; Lovell, S.; Battaile, K. P.; Im, W.; Rivera, M. Concerted motions networking pores and distant ferroxidase centers enable bacterioferritin function and iron traffic. *Biochemistry* **2015**, *54* (8), 1611−27.

(95) Kasyutich, O.; Ilari, A.; Fiorillo, A.; Tatchev, D.; Hoell, A.; Ceci, P. Silver ion incorporation and nanoparticle formation inside the cavity of Pyrococcus furiosus ferritin: structural and size-distribution analyses. *J. Am. Chem. Soc.* **2010**, *132* (10), 3621−7.

(96) Huard, D. J. E.; Kane, K. M.; Tezcan, F. A. Re-engineering protein interfaces yields copper-inducible ferritin cage assembly. *Nature Chemical Biology* **2013**, *9* (3), 169−176.

(97) Calisti, L.; Trabuco, M. C.; Boffi, A.; Testi, C.; Montemiglio, L. C.; des Georges, A.; Benni, I.; Ilari, A.; Taciak, B.; Bialasek, M.; Rygiel, T.; Krol, M.; Baiocco, P.; Bonamore, A. Engineered ferritin for lanthanide binding. *PloS one* **2018**, *13* (8), No. e0201859.

(98) Si, K.; Ming, T.; Li, Y.; Qiu, X.; Chen, L.; Zhou, J.; Lu, C.; Su, X.; Li, Y.; Cheong, L.-Z. Heavy metal detoxification by recombinant ferritin from Apostichopus japonicus. *RSC Advances* **2017**, *7* (66), 41909−41918.

(99) Taher, M.; Maity, B.; Nakane, T.; Abe, S.; Ueno, T.; Mazumdar, S. Controlled Uptake of an Iridium Complex inside Engineered apo-Ferritin Nanocages: Study of Structure and Catalysis**. *Angewandte Chemie International Edition* **2022**, No. e202116623.

(100) Saldan, I.; Semenyuk, Y.; Marchuk, I.; Reshetnyak, O. Chemical synthesis and application of palladium nanoparticles. *J. Mater. Sci.* **2015**, *50* (6), 2337−2354.

(101) Kanbak-Aksu, S.; Nahid Hasan, M.; Hagen, W. R.; Hollmann, F.; Sordi, D.; Sheldon, R. A.; Arends, I. W. Ferritin-supported palladium nanoclusters: selective catalysts for aerobic oxidations in water. *Chem Commun (Camb)* **2012**, *48* (46), 5745−7.

(102) Ueno, T.; Suzuki, M.; Goto, T.; Matsumoto, T.; Nagayama, K.; Watanabe, Y. Size-selective olefin hydrogenation by a Pd nanocluster provided in an apo-ferritin cage. *Angew. Chem.* **2004**, *43* (19), 2527−30.

(103) Ueno, T.; Abe, M.; Hirata, K.; Abe, S.; Suzuki, M.; Shimizu, N.; Yamamoto, M.; Takata, M.; Watanabe, Y. Process of Accumulation of Metal Ions on the Interior Surface of apo-Ferritin: Crystal Structures of a Series of apo-Ferritins Containing Variable Quantities of Pd(II) Ions. *J. Am. Chem. Soc.* **2009**, *131* (14), 5094−5100.

(104) Suzuki, M.; Abe, M.; Ueno, T.; Abe, S.; Goto, T.; Toda, Y.; Akita, T.; Yamada, Y.; Watanabe, Y. Preparation and catalytic reaction of Au/Pd bimetallic nanoparticles in Apo-ferritin. *Chemical Communications* **2009**, *32*, 4871−4873.

(105) Zheng, B.; Yamashita, I.; Uenuma, M.; Iwahori, K.; Kobayashi, M.; Uraoka, Y. Site-directed delivery of ferritin-encapsulated gold nanoparticles. *Nanotechnology* **2010**, *21* (4), 045305.

(106) Fan, R.; Chew, S. W.; Cheong, V. V.; Orner, B. P. Fabrication of Gold Nanoparticles Inside Unmodified Horse Spleen Apoferritin. *Small* **2010**, *6* (14), 1483−1487.

(107) Sun, C.; Yang, H.; Yuan, Y.; Tian, X.; Wang, L.; Guo, Y.; Xu, L.; Lei, J.; Gao, N.; Anderson, G. J.; Liang, X.-J.; Chen, C.; Zhao, Y.; Nie, G. Controlling Assembly of Paired Gold Clusters within Apoferritin Nanoreactor for in Vivo Kidney Targeting and Biomedical Imaging. *J. Am. Chem. Soc.* **2011**, *133* (22), 8617−8624.

(108) Butts, C. A.; Swift, J.; Kang, S.-g.; Di Costanzo, L.; Christianson, D. W.; Saven, J. G.; Dmochowski, I. J. Directing Noble Metal Ion Chemistry within a Designed Ferritin Protein. *Biochemistry* **2008**, *47* (48), 12729−12739.

(109) Maity, B.; Abe, S.; Ueno, T. Observation of gold sub-nanocluster nucleation within a crystalline protein cage. *Nat. Commun.* **2017**, *8*, 14820.

(110) Tosha, T.; Behera, R. K.; Ng, H. L.; Bhattasali, O.; Alber, T.; Theil, E. C. Ferritin protein nanocage ion channels: gating by N-terminal extensions. *The Journal of biological chemistry* **2012**, *287* (16), 13016−25.

(111) Chan, W. C. W.; Maxwell, D. J.; Gao, X.; Bailey, R. E.; Han, M.; Nie, S. Luminescent quantum dots for multiplexed biological detection and imaging. *Curr. Opin. Biotechnol.* **2002**, *13*, 40−46.

(112) Drbohlavova, J.; Adam, V.; Kizek, R.; Hubalek, J. Quantum dots - characterization, preparation and usage in biological systems. *Int J Mol Sci* **2009**, *10* (2), 656−673.

(113) Fontes, A.; Santos, B. *Quantum Dots: Applications in Biology*, 2nd ed.; Humana Press: New York, 2014; p XI, 258.

(114) Bera, D.; Qian, L.; Tseng, T.-K.; Holloway, P. H. Quantum Dots and Their Multimodal Applications: A Review. *Materials* **2010**, *3* (4), 2260.

(115) Kargozar, S.; Hoseini, S. J.; Milan, P. B.; Hooshmand, S.; Kim, H.-W.; Mozafari, M. Quantum Dots: A Review from Concept to Clinic. *Biotechnology Journal* **2020**, *15* (12), 2000117.

(116) Murray, C. B.; Kagan, C. R.; Bawendi, M. G. Synthesis and Characterization of Monodisperse Nanocrystals and Close-Packed Nanocrystal Assemblies. *Annu. Rev. Mater. Sci.* **2000**, *30* (1), 545−610.

(117) Onyia, A.; Ikeri, H.; Nwobodo, A. Theoretical study of the quantum confinement effects on quantum dots using particle in a box model. *Journal of Ovonic Research* **2018**, *14* (1), 49−54.

(118) Valizadeh, A.; Mikaeili, H.; Samiei, M.; Farkhani, S. M.; Zarghami, N.; Kouhi, M.; Akbarzadeh, A.; Davaran, S. Quantum dots: synthesis, bioapplications, and toxicity. *Nanoscale Res. Lett.* **2012**, *7* (1), 480.

(119) Chukwuocha, E. O.; Onyeaju, M. C.; Harry, T. S. T. Theoretical Studies on the Effect of Confinement on Quantum Dots Using the Brus Equation. *World Journal of Condensed Matter Physics* **2012**, *02* (02), 96−100.

(120) Ramirez, H. Y.; Lin, C. H.; Chao, C. C.; Hsu, Y.; You, W. T.; Huang, S. Y.; Chen, Y. T.; Tseng, H. C.; Chang, W. H.; Lin, S. D.; Cheng, S. J. Optical fine structures of highly quantized InGaAs/GaAs self-assembled quantum dots. *Physical Review B* **2010**, *81* (24), 245324.

(121) Ulbricht, R.; Pijpers, J. J. H.; Groeneveld, E.; Koole, R.; Donega, C. d. M.; Vanmaekelbergh, D.; Delerue, C.; Allan, G.; Bonn, M. Loosening Quantum Confinement: Observation of Real Conductivity Caused by Hole Polarons in Semiconductor Nanocryst-als Smaller than the Bohr Radius. *Nano Letters* **2012**, *12* (9), 4937−4942.

(122) Brichkin, S. B.; Razumov, V. F. Colloidal quantum dots: synthesis, properties and applications. *Russ. Chem. Rev.* **2016**, *85* (12), 1297−1312.

(123) Shao, L.; Gao, Y.; Yan, F. Semiconductor Quantum Dots for Biomedicial Applications. *Sensors* **2011**, *11* (12), 11736.

(124) Han, M.; Gao, X.; Su, J. Z.; Nie, S. Quantum-dot-tagged microbeads for multiplexed optical coding of biomolecules. *Nat. Biotechnol.* **2001**, *19* (7), 631−635.

(125) Murray, C. B.; Norris, D. J.; Bawendi, M. G. Synthesis and characterization of nearly monodisperse CdE (E = sulfur, selenium, tellurium) semiconductor nanocrystallites. *J. Am. Chem. Soc.* **1993**, *115* (19), 8706−8715.

(126) Dabbousi, B. O.; Rodriguez-Viejo, J.; Mikulec, F. V.; Heine, J. R.; Mattoussi, H.; Ober, R.; Jensen, K. F.; Bawendi, M. G. (CdSe)ZnS Core-Shell Quantum Dots: Synthesis and Characterization of a Size Series of Highly Luminescent Nanocrystallites. *The Journal of Physical Chemistry B* **1997**, *101* (46), 9463−9475.

(127) Peng, X.; Schlamp, M. C.; Kadavanich, A. V.; Alivisatos, A. P. Epitaxial Growth of Highly Luminescent CdSe/CdS Core/Shell Nanocrystals with Photostability and Electronic Accessibility. *J. Am. Chem. Soc.* **1997**, *119* (30), 7019−7029.

(128) Hines, M. A.; Guyot-Sionnest, P. Synthesis and Characterization of Strongly Luminescing ZnS-Capped CdSe Nanocrystals. *The Journal of Physical Chemistry* **1996**, *100* (2), 468−471.

(129) Peng, X.; Wickham, J.; Alivisatos, A. P. Kinetics of II−VI and III−V Colloidal Semiconductor Nanocrystal Growth: "Focusing" of Size Distributions. *J. Am. Chem. Soc.* **1998**, *120* (21), 5343−5344.

(130) De Smet, Y.; Deriemaeker, L.; Parloo, E.; Finsy, R. On the Determination of Ostwald Ripening Rates from Dynamic Light Scattering Measurements. *Langmuir* **1999**, *15* (7), 2327−2332.

(131) Maronesi, R. N.; Ferreira, D. L.; Lana, M. L.; Couto, M. S.; Ferreira, S. O.; Silva, A. G. A facile synthesis route for preparing aqueous colloidal CdS quantum dots with size-tunable optical properties. *J. Lumin.* **2018**, *202*, 489−496.

(132) Chien, C. Y.; Lai, W. T.; Chang, Y. J.; Wang, C. C.; Kuo, M. H.; Li, P. W. Size tunable Ge quantum dots for near-ultraviolet to near-infrared photosensing with high figures of merit. *Nanoscale* **2014**, *6* (10), 5303−5308.

(133) Hines, M. A.; Guyot-Sionnest, P. Bright UV-Blue Luminescent Colloidal ZnSe Nanocrystals. *The Journal of Physical Chemistry B* **1998**, *102* (19), 3655−3657.

(134) Mićić, O. I.; Cheong, H. M.; Fu, H.; Zunger, A.; Sprague, J. R.; Mascarenhas, A.; Nozik, A. J. Size-Dependent Spectroscopy of InP Quantum Dots. *The Journal of Physical Chemistry B* **1997**, *101* (25), 4904−4912.

(135) Chen, H.; Gai, H.; Yeung, E. S. Inhibition of photobleaching and blue shift in quantum dots. *Chemical Communications* **2009**, *13*, 1676−1678.

(136) Zhu, S.; Zhang, J.; Qiao, C.; Tang, S.; Li, Y.; Yuan, W.; Li, B.; Tian, L.; Liu, F.; Hu, R.; Gao, H.; Wei, H.; Zhang, H.; Sun, H.; Yang, B. Strongly green-photoluminescent graphene quantum dots for bioimaging applications. *Chemical Communications* **2011**, *47* (24), 6858−6860.

(137) Kairdolf, B. A.; Smith, A. M.; Stokes, T. H.; Wang, M. D.; Young, A. N.; Nie, S. Semiconductor Quantum Dots for Bioimaging and Biodiagnostic Applications. *Annual Review of Analytical Chemistry* **2013**, *6* (1), 143−162.

(138) Kumar, U.; Kumari, K.; Sharma, S. N.; Kumar, M.; Vankar, V. D.; Kakkar, R.; Kumar, V. Role of surface modification of colloidal CdSe quantum dots on the properties of hybrid organic−inorganic nanocomposites. *Colloid Polym. Sci.* **2010**, *288* (8), 841−849.

(139) Ren, Z.; Yu, J.; Pan, Z.; Wang, J.; Zhong, X. Inorganic Ligand Thiosulfate-Capped Quantum Dots for Efficient Quantum Dot Sensitized Solar Cells. *ACS Applied Materials & Interfaces* **2017**, *9* (22), 18936−18944.

(140) Cordones, A. A.; Scheele, M.; Alivisatos, A. P.; Leone, S. R. Probing the Interaction of Single Nanocrystals with Inorganic Capping Ligands: Time-Resolved Fluorescence from CdSe−CdS Quantum Dots Capped with Chalcogenidometalates. *J. Am. Chem. Soc.* **2012**, *134* (44), 18366−18373.

(141) Wagner, A. M.; Knipe, J. M.; Orive, G.; Peppas, N. A. Quantum dots in biomedical applications. *Acta Biomaterialia* **2019**, *94*, 44−63.

(142) Klostranec, J. M.; Chan, W. C. W. Quantum Dots in Biological and Biomedical Research: Recent Progress and Present Challenges. *Adv. Mater.* **2006**, *18* (15), 1953−1964.

(143) He, X.; Ma, N. An overview of recent advances in quantum dots for biomedical applications. *Colloids and Surfaces B: Biointerfaces* **2014**, *124*, 118−131.

(144) Selopal, G. S.; Zhao, H.; Wang, Z. M.; Rosei, F. Core/Shell Quantum Dots Solar Cells. *Advanced Functional Materials* **2020**, *30* (13), 1908762.

(145) Kim, H.; Han, J. Y.; Kang, D. S.; Kim, S. W.; Jang, D. S.; Suh, M.; Kirakosyan, A.; Jeon, D. Y. Characteristics of CuInS2/ZnS quantum dots and its application on LED. *J. Cryst. Growth* **2011**, *326* (1), 90−93.

(146) Bimberg, D. Quantum dots for lasers, amplifiers and computing. *Journal of Physics D: Applied Physics* **2005**, *38* (13), 2055−2058.

(147) Ren, B.-C.; Deng, F.-G. Hyper-parallel photonic quantum computation with coupled quantum dots. *Sci. Rep.* **2015**, *4*, 4623.

(148) Hildebrandt, N. Biofunctional Quantum Dots: Controlled Conjugation for Multiplexed Biosensors. *ACS Nano* **2011**, *5* (7), 5286−5290.

(149) Smith, A. M.; Duan, H.; Mohs, A. M.; Nie, S. Bioconjugated quantum dots for in vivo molecular and cellular imaging. *Adv. Drug Delivery Rev.* **2008**, *60* (11), 1226−1240.

(150) Peng, H.; Zhang, L.; Kjallman, T. H. M.; Soeller, C.; Travas-Sejdic, J. DNA Hybridization Detection with Blue Luminescent Quantum Dots and Dye-Labeled Single-Stranded DNA. *J. Am. Chem. Soc.* **2007**, *129* (11), 3048−3049.

(151) Zhao, L.; Cheng, P.; Li, J.; Zhang, Y.; Gu, M.; Liu, J.; Zhang, J.; Zhu, J.-J. Analysis of Nonadherent Apoptotic Cells by a Quantum Dots Probe in a Microfluidic Device for Drug Screening. *Anal. Chem.* **2009**, *81* (16), 7075−7080.

(152) Rhyner, M. N.; Smith, A. M.; Gao, X.; Mao, H.; Yang, L.; Nie, S. Quantum dots and multifunctional nanoparticles: new contrast agents for tumor imaging. *Nanomedicine* **2006**, *1* (2), 209−217.

(153) Xu, G.; Zeng, S.; Zhang, B.; Swihart, M. T.; Yong, K.-T.; Prasad, P. N. New Generation Cadmium-Free Quantum Dots for Biophotonics and Nanomedicine. *Chemical Reviews* **2016**, *116* (19), 12234−12327.

(154) Liu, H.; Zhang, X.; Xing, B.; Han, P.; Gambhir, S. S.; Cheng, Z. Radiation-Luminescence-Excited Quantum Dots for in vivo Multiplexed Optical Imaging. *Small* **2010**, *6* (10), 1087−1091.

(155) Xie, H.; Liu, M.; You, B.; Luo, G.; Chen, Y.; Liu, B.; Jiang, Z.; Chu, P. K.; Shao, J.; Yu, X.-F. Biodegradable Bi2O2Se Quantum Dots for Photoacoustic Imaging-Guided Cancer Photothermal Therapy. *Small* **2020**, *16* (1), 1905208.

(156) Li, J.; Zhu, J.-J. Quantum dots for fluorescent biosensing and bio-imaging applications. *Analyst* **2013**, *138* (9), 2506−2515.

(157) Lane, L. A.; Smith, A. M.; Lian, T.; Nie, S. Compact and Blinking-Suppressed Quantum Dots for Single-Particle Tracking in Live Cells. *The Journal of Physical Chemistry B* **2014**, *118* (49), 14140−14147.

(158) Chu, M.; Pan, X.; Zhang, D.; Wu, Q.; Peng, J.; Hai, W. The therapeutic efficacy of CdTe and CdSe quantum dots for photo-thermal cancer therapy. *Biomaterials* **2012**, *33* (29), 7071−7083.

(159) Jing, L.; Ding, K.; Kershaw, S. V.; Kempson, I. M.; Rogach, A. L.; Gao, M. Magnetically Engineered Semiconductor Quantum Dots as Multimodal Imaging Probes. *Adv. Mater.* **2014**, *26* (37), 6367−6386.

(160) Fang, M.; Peng, C.-W.; Pang, D.-W.; Li, Y. Quantum dots for cancer research: current status, remaining issues, and future perspectives. *Cancer Biol. Med.* **2012**, *9* (3), 151−163.

(161) Azzazy, H. M. E.; Mansour, M. M. H.; Kazmierczak, S. C. From diagnostics to therapy: Prospects of quantum dots. *Clinical Biochemistry* **2007**, *40* (13), 917−927.

(162) Fu, Y.; Jang, M.-S.; Wu, T.; Lee, J. H.; Li, Y.; Lee, D. S.; Yang, H. Y. Multifunctional hyaluronic acid-mediated quantum dots for targeted intracellular protein delivery and real-time fluorescence imaging. *Carbohydr. Polym.* **2019**, *224*, 115174.

(163) Chen, B.; Liu, Q.; Zhang, Y.; Xu, L.; Fang, X. Transmembrane Delivery of the Cell-Penetrating Peptide Conjugated Semiconductor Quantum Dots. *Langmuir* 2008, 24 (20), 11866−11871.

(164) Wang, X.; Sun, X.; Lao, J.; He, H.; Cheng, T.; Wang, M.; Wang, S.; Huang, F. Multifunctional graphene quantum dots for simultaneous targeted cellular imaging and drug delivery. *Colloids and Surfaces B: Biointerfaces* 2014, 122, 638−644.

(165) Li, Y.; Li, Z.; Wang, X.; Liu, F.; Cheng, Y.; Zhang, B.; Shi, D. In vivo cancer targeting and imaging-guided surgery with near infrared-emitting quantum dot bioconjugates. *Theranostics* 2012, 2 (8), 769−776.

(166) Rezaei, A.; Hashemi, E. A pseudohomogeneous nanocarrier based on carbon quantum dots decorated with arginine as an efficient gene delivery vehicle. *Sci. Rep.* 2021, 11, 13790.

(167) Chen, N.; He, Y.; Su, Y.; Li, X.; Huang, Q.; Wang, H.; Zhang, X.; Tai, R.; Fan, C. The cytotoxicity of cadmium-based quantum dots. *Biomaterials* 2012, 33 (5), 1238−1244.

(168) Shiohara, A.; Hoshino, A.; Hanaki, K.-i.; Suzuki, K.; Yamamoto, K. On the Cyto-Toxicity Caused by Quantum Dots. *Microbiol. Immunol.* 2004, 48 (9), 669−675.

(169) Wu, T.; Tang, M. Toxicity of quantum dots on respiratory system. *Inhalation Toxicology* 2014, 26 (2), 128−139.

(170) Tsoi, K. M.; Dai, Q.; Alman, B. A.; Chan, W. C. W. Are Quantum Dots Toxic? Exploring the Discrepancy Between Cell Culture and Animal Studies. *Acc. Chem. Res.* 2013, 46 (3), 662−671.

(171) Sun, H.; Zhang, F.; Wei, H.; Yang, B. The effects of composition and surface chemistry on the toxicity of quantum dots. *Journal of Materials Chemistry B* 2013, 1 (47), 6485−6494.

(172) Hezinger, A. F. E.; Teßmar, J.; Göpferich, A. Polymer coating of quantum dots − A powerful tool toward diagnostics and sensorics. *European Journal of Pharmaceutics and Biopharmaceutics* 2008, 68 (1), 138−152.

(173) Wang, Y.; Hu, R.; Lin, G.; Roy, I.; Yong, K.-T. Functionalized Quantum Dots for Biosensing and Bioimaging and Concerns on Toxicity. *ACS Applied Materials & Interfaces* 2013, 5 (8), 2786−2799.

(174) Lagerholm, B. C.; Wang, M.; Ernst, L. A.; Ly, D. H.; Liu, H.; Bruchez, M. P.; Waggoner, A. S. Multicolor Coding of Cells with Cationic Peptide Coated Quantum Dots. *Nano Letters* 2004, 4 (10), 2019−2022.

(175) Xing, R.; Wang, X.; Yan, L.; Zhang, C.; Yang, Z.; Wang, X.; Guo, Z. Fabrication of water soluble and biocompatible CdSe nanoparticles in apoferritin with the aid of EDTA. *Dalton Trans.* 2009, 1710−1713.

(176) Bradshaw, T. D.; Junor, M.; Patanè, A.; Clarke, P.; Thomas, N. R.; Li, M.; Mann, S.; Turyanska, L. Apoferritin-encapsulated PbS quantum dots significantly inhibit growth of colorectal carcinoma cells. *Journal of Materials Chemistry B* 2013, 1 (45), 6254−6260.

(177) Wong, K. K. W.; Mann, S. Biomimetic synthesis of cadmium sulfide-ferritin nanocomposites. *Adv. Mater.* 1996, 8 (11), 928−932.

(178) Yamashita, I.; Hayashi, J.; Hara, M. Bio-template Synthesis of Uniform CdSe Nanoparticles Using Cage-shaped Protein, Apoferritin. *Chem. Lett.* 2004, 33 (9), 1158−1159.

(179) Iwahori, K.; Yamashita, I. Fabrication of CdS nanoparticles in the bio-template, apoferritin cavity by a slow chemical reaction system. *Journal of Physics: Conference Series* 2007, 61, 492.

(180) Iwahori, K.; Yamashita, I. Size-controlled one-pot synthesis of fluorescent cadmium sulfide semiconductor nanoparticles in an apoferritin cavity. *Nanotechnology* 2008, 19 (49), 495601.

(181) Iwahori, K.; Yoshizawa, K.; Muraoka, M.; Yamashita, I. Fabrication of ZnSe Nanoparticles in the Apoferritin Cavity by Designing a Slow Chemical Reaction System. *Inorganic Chemistry* 2005, 44 (18), 6393−6400.

(182) Naito, M.; Iwahori, K.; Miura, A.; Yamane, M.; Yamashita, I. Circularly Polarized Luminescent CdS Quantum Dots Prepared in a Protein Nanocage. *Angew. Chem., Int. Ed.* 2010, 49, 7006−7009.

(183) Selvan, S. T.; Tan, T. T.; Ying, J. Y. Robust, Non-Cytotoxic, Silica-Coated CdSe Quantum Dots with Efficient Photoluminescence. *Adv. Mater.* 2005, 17 (13), 1620−1625.

(184) Derfus, A. M.; Chan, W. C. W.; Bhatia, S. N. Probing the Cytotoxicity of Semiconductor Quantum Dots. *Nano Letters* 2004, 4 (1), 11−18.

(185) Lim, Y. T.; Kim, S.; Nakayama, A.; Stott, N. E.; Bawendi, M. G.; Frangioni, J. V. Selection of quantum dot wavelengths for biomedical assays and imaging. *Mol Imaging* 2003, 2 (1), 50−64.

(186) Turyanska, L.; Bradshaw, T. D.; Sharpe, J.; Li, M.; Mann, S.; Thomas, N. R.; Patane, A. The Biocompatibility of Apoferritin-Encapsulated PbS Quantum Dots. *Small* 2009, 5, 1738−1741.

(187) Hennequin, B.; Turyanska, L.; Ben, T.; Beltrán, A. M.; Molina, S. I.; Li, M.; Mann, S.; Patanè, A.; Thomas, N. R. Aqueous Near-Infrared Fluorescent Composites Based on Apoferritin-Encapsulated PbS Quantum Dots. *Adv. Mater.* 2008, 20 (19), 3592−3596.

(188) Wong, K. K.; Colfen, H.; Whilton, N. T.; Douglas, T.; Mann, S. Synthesis and characterization of hydrophobic ferritin proteins. *J Inorg Biochem* 1999, 76 (3−4), 187−95.

(189) Nasrollahi, F.; Sana, B.; Paramelle, D.; Ahadian, S.; Khademhosseini, A.; Lim, S. Incorporation of Graphene Quantum Dots, Iron, and Doxorubicin in/on Ferritin Nanocages for Bimodal Imaging and Drug Delivery. *Advanced Therapeutics* 2020, 3 (3), 1900183.

(190) Wang, J.; Qiu, J. A review of carbon dots in biological applications. *J. Mater. Sci.* 2016, 51 (10), 4728−4738.

(191) Chinnathambi, S.; Chen, S.; Ganesan, S.; Hanagata, N. Silicon Quantum Dots for Biological Applications. *Advanced Healthcare Materials* 2014, 3 (1), 10−29.

(192) Gu, Y.-P.; Cui, R.; Zhang, Z.-L.; Xie, Z.-X.; Pang, D.-W. Ultrasmall Near-Infrared Ag2Se Quantum Dots with Tunable Fluorescence for in Vivo Imaging. *J. Am. Chem. Soc.* 2012, 134 (1), 79−82.

(193) Ding, C.; Huang, Y.; Shen, Z.; Chen, X. Synthesis and Bioapplications of Ag2S Quantum Dots with Near-Infrared Fluorescence. *Adv. Mater.* 2021, 33 (32), 2007768.

(194) Durán, N.; Simões, M. B.; de Moraes, A. C. M.; Fávaro, W. J.; Seabra, A. B. Nanobiotechnology of Carbon Dots: A Review. *Journal of Biomedical Nanotechnology* 2016, 12 (7), 1323−1347.

(195) Bhattacharya, A.; Chatterjee, S.; Prajapati, R.; Mukherjee, T. K. Size-dependent penetration of carbon dots inside the ferritin nanocages: evidence for the quantum confinement effect in carbon dots. *Phys. Chem. Chem. Phys.* 2015, 17, 12833−12840.

(196) Pullin, J.; Bradley, J. M.; Moore, G. R.; Le Brun, N. E.; Wilson, M. T.; Svistunenko, D. A. Electron Transfer from Haem to the Di-Iron Ferroxidase Centre in Bacterioferritin. *Angewandte Chemie International Edition* 2021, 60 (15), 8376−8379.

(197) Hansen, K. R.; Peterson, J. R.; Perego, A.; Shelley, M.; Olsen, C. R.; Perez, L. D.; Hogg, H. L.; Watt, R. K.; Colton, J. S. Lead sulfide quantum dots inside ferritin: synthesis and application to photovoltaics. *Applied Nanoscience* 2018, 8 (7), 1687−1699.

(198) Quinto, C. A.; Mohindra, P.; Tong, S.; Bao, G. Multifunctional superparamagnetic iron oxide nanoparticles for combined chemotherapy and hyperthermia cancer treatment. *Nanoscale* 2015, 7 (29), 12728−12736.

(199) Eslaminejad, T.; Nematollahi-Mahani, S. N.; Ansari, M. Glioblastoma Targeted Gene Therapy Based on pEGFP/p53-Loaded Superparamagnetic Iron Oxide Nanoparticles. *Current Gene Therapy* 2017, 17 (1), 59−69.

(200) Laurent, S.; Saei, A. A.; Behzadi, S.; Panahifar, A.; Mahmoudi, M. Superparamagnetic iron oxide nanoparticles for delivery of therapeutic agents: opportunities and challenges. *Expert Opinion on Drug Delivery* 2014, 11 (9), 1449−1470.

(201) Zhao, X.; Zhao, H.; Chen, Z.; Lan, M. Ultrasmall Superparamagnetic Iron Oxide Nanoparticles for Magnetic Resonance Imaging Contrast Agent. *Journal of Nanoscience and Nanotechnology* 2014, 14 (1), 210−220.

(202) Wang, Y.; Xu, C.; Chang, Y.; Zhao, L.; Zhang, K.; Zhao, Y.; Gao, F.; Gao, X. Ultrasmall Superparamagnetic Iron Oxide Nanoparticle for T2-Weighted Magnetic Resonance Imaging. *ACS Applied Materials & Interfaces* 2017, 9 (34), 28959−28966.

(203) Chen, C.; Ge, J.; Gao, Y.; Chen, L.; Cui, J.; Zeng, J.; Gao, M. Ultrasmall superparamagnetic iron oxide nanoparticles: A next generation contrast agent for magnetic resonance imaging. *WIREs Nanomed. Nanobiotechnol.* 2022, *14*, No. e1740.

(204) Samrot, A. V.; Sahithya, C. S.; Selvarani A, J.; Purayil, S. K.; Ponnaiah, P. A review on synthesis, characterization and potential biological applications of superparamagnetic iron oxide nanoparticles. *Current Research in Green and Sustainable Chemistry* 2021, *4*, 100042.

(205) Dulińska-Litewka, J.; Łazarczyk, A.; Hałubiec, P.; Szafrański, O.; Karnas, K.; Karewicz, A. Superparamagnetic Iron Oxide Nanoparticles—Current and Prospective Medical Applications. *Materials* 2019, *12* (4), 617.

(206) Wang, A. Z.; Bagalkot, V.; Vasilliou, C. C.; Gu, F.; Alexis, F.; Zhang, L.; Shaikh, M.; Yuet, K.; Cima, M. J.; Langer, R.; Kantoff, P. W.; Bander, N. H.; Jon, S.; Farokhzad, O. C. Superparamagnetic iron oxide nanoparticle-aptamer bioconjugates for combined prostate cancer imaging and therapy. *ChemMedChem* 2008, *3* (9), 1311–1315.

(207) Mahmoudi, M.; Simchi, A.; Imani, M.; Milani, A. S.; Stroeve, P. Optimal Design and Characterization of Superparamagnetic Iron Oxide Nanoparticles Coated with Polyvinyl Alcohol for Targeted Delivery and Imaging. *The Journal of Physical Chemistry B* 2008, *112* (46), 14470–14481.

(208) Li, L.; Gao, F.; Jiang, W.; Wu, X.; Cai, Y.; Tang, J.; Gao, X.; Gao, F. Folic acid-conjugated superparamagnetic iron oxide nanoparticles for tumor-targeting MR imaging. *Drug Delivery* 2016, *23* (5), 1726–1733.

(209) Kemikli, N.; Kavas, H.; Kazan, S.; Baykal, A.; Ozturk, R. Synthesis of protoporphyrin coated superparamagnetic iron oxide nanoparticles via dopamine anchor. *J. Alloys Compd.* 2010, *502* (2), 439–444.

(210) Lee, H.; Lee, E.; Kim, D. K.; Jang, N. K.; Jeong, Y. Y.; Jon, S. Antibiofouling Polymer-Coated Superparamagnetic Iron Oxide Nanoparticles as Potential Magnetic Resonance Contrast Agents for in Vivo Cancer Imaging. *J. Am. Chem. Soc.* 2006, *128* (22), 7383–7389.

(211) Yang, L.; Fu, S.; Cai, Z.; Liu, L.; Xia, C.; Gong, Q.; Song, B.; Ai, H. Integration of PEG-conjugated gadolinium complex and superparamagnetic iron oxide nanoparticles as T1–T2 dual-mode magnetic resonance imaging probes. *Regenerative Biomaterials* 2021, *8* (6), No. rbab064.

(212) de Espindola, A.; Chagas, C. S.; Barbosa, E.; Castro, C. E.; Fonseca, F. L. A.; Haddad, P. S.; Molina, C. Luminescent − Superparamagnetic iron oxide nanoparticles functionalized with biomolecules and lanthanides ions. Potential platforms for theranostic applications. *Journal of Magnetism and Magnetic Materials* 2022, *545*, 168751.

(213) Wang, J.; Zhang, B.; Yang, G.; Su, L.; Wang, L.; Gao, F. Transferrin-Conjugated Superparamagnetic Iron Oxide Nanoparticles as In Vivo Magnetic Resonance Imaging Contrast Agents. *Journal of Nanoscience and Nanotechnology* 2020, *20* (4), 2018–2024.

(214) Santoyo Salazar, J.; Perez, L.; de Abril, O.; Truong Phuoc, L.; Ihiawakrim, D.; Vazquez, M.; Greneche, J.-M.; Begin-Colin, S.; Pourroy, G. Magnetic Iron Oxide Nanoparticles in 10−40 nm Range: Composition in Terms of Magnetite/Maghemite Ratio and Effect on the Magnetic Properties. *Chem. Mater.* 2011, *23* (6), 1379–1386.

(215) Singh, N.; Jenkins, G. J. S.; Asadi, R.; Doak, S. H. Potential toxicity of superparamagnetic iron oxide nanoparticles (SPION). *Nano Reviews* 2010, *1* (1), 5358.

(216) Mahmoudi, M.; Hofmann, H.; Rothen-Rutishauser, B.; Petri-Fink, A. Assessing the In Vitro and In Vivo Toxicity of Superparamagnetic Iron Oxide Nanoparticles. *Chemical Reviews* 2012, *112* (4), 2323–2338.

(217) Cai, H.; An, X.; Cui, J.; Li, J.; Wen, S.; Li, K.; Shen, M.; Zheng, L.; Zhang, G.; Shi, X. Facile Hydrothermal Synthesis and Surface Functionalization of Polyethyleneimine-Coated Iron Oxide Nanoparticles for Biomedical Applications. *ACS Applied Materials & Interfaces* 2013, *5* (5), 1722–1731.

(218) Bomatí-Miguel, O.; Tartaj, P.; Morales, M. P.; Bonville, P.; Golla-Schindler, U.; Zhao, X. Q.; Veintemillas-Verdaguer, S. Core−

(219) Besenhard, M. O.; LaGrow, A. P.; Hodzic, A.; Kriechbaum, M.; Panariello, L.; Bais, G.; Loizou, K.; Damilos, S.; Margarida Cruz, M.; Thanh, N. T. K.; Gavriilidis, A. Co-precipitation synthesis of stable iron oxide nanoparticles with NaOH: New insights and continuous production via flow chemistry. *Chemical Engineering Journal* 2020, *399*, 125740.

(220) Lei, P.; Boies, A. M.; Calder, S.; Girshick, S. L. Thermal Plasma Synthesis of Superparamagnetic Iron Oxide Nanoparticles. *Plasma Chemistry and Plasma Processing* 2012, *32* (3), 519−531.

(221) Kayani, Z. N.; Arshad, S.; Riaz, S.; Naseem, S. Synthesis of Iron Oxide Nanoparticles by Sol−Gel Technique and Their Characterization. *IEEE Trans. Magn.* 2014, *50* (8), 1−4.

(222) Hui, B. H.; Salimi, M. N. Production of Iron Oxide Nanoparticles by Co-Precipitation method with Optimization Studies of Processing Temperature, pH and Stirring Rate. *IOP Conference Series: Materials Science and Engineering* 2020, *743* (1), 012036.

(223) Unni, M.; Uhl, A. M.; Savliwala, S.; Savitzky, B. H.; Dhavalikar, R.; Garraud, N.; Arnold, D. P.; Kourkoutis, L. F.; Andrew, J. S.; Rinaldi, C. Thermal Decomposition Synthesis of Iron Oxide Nanoparticles with Diminished Magnetic Dead Layer by Controlled Addition of Oxygen. *ACS Nano* 2017, *11* (2), 2284−2303.

(224) Cotin, G.; Kiefer, C.; Perton, F.; Ihiawakrim, D.; Blanco-Andujar, C.; Moldovan, S.; Lefevre, C.; Ersen, O.; Pichon, B.; Mertz, D.; Bégin-Colin, S. Unravelling the Thermal Decomposition Parameters for The Synthesis of Anisotropic Iron Oxide Nanoparticles. *Nanomaterials* 2018, *8* (11), 881.

(225) Teng, X.; Yang, H. Effects of surfactants and synthetic conditions on the sizes and self-assembly of monodisperse iron oxide nanoparticles. *Journal of Materials Chemistry* 2004, *14* (4), 774−779.

(226) Wang, Z.; Lam, A.; Acosta, E. Suspensions of Iron Oxide Nanoparticles Stabilized by Anionic Surfactants. *Journal of Surfactants and Detergents* 2013, *16* (3), 397−407.

(227) Cui, H.; Liu, Y.; Ren, W. Structure switch between α-Fe2O3, γ-Fe2O3 and Fe3O4 during the large scale and low temperature sol−gel synthesis of nearly monodispersed iron oxide nanoparticles. *Advanced Powder Technology* 2013, *24* (1), 93−97.

(228) Jitianu, A.; Crisan, M.; Meghea, A.; Rau, I.; Zaharescu, M. Influence of the silica based matrix on the formation of iron oxide nanoparticles in the Fe2O3−SiO2 system, obtained by sol−gel method. *Journal of Materials Chemistry* 2002, *12* (5), 1401−1407.

(229) Banerjee, I.; Joshi, N. K.; Sahasrabudhe, S. N.; Kulkarni, N. V.; Karmakar, S.; Pasricha, R.; Ghorui, S.; Tak, A. K.; Murthy, S. P. S. S.; Bhoraskar, S. V.; Das, A. K. In Situ Optical Emission Spectroscopic Investigations During Arc Plasma Synthesis of Iron Oxide Nanoparticles by Thermal Plasma. *IEEE Transactions on Plasma Science* 2006, *34* (4), 1175−1182.

(230) Raut, S. A.; Mutadak, P. R.; Kumar, S.; Kanhe, N. S.; Huprikar, S.; Pol, H. V.; Phase, D. M.; Bhoraskar, S. V.; Mathe, V. L. Single step, phase controlled, large scale synthesis of ferrimagnetic iron oxide polymorph nanoparticles by thermal plasma route and their rheological properties. *Journal of Magnetism and Magnetic Materials* 2018, *449*, 232−242.

(231) Koushika, E. M.; Shanmugavelayutham, G.; Saravanan, P.; Balasubramanian, C. Rapid synthesis of nano-magnetite by thermal plasma route and its magnetic properties. *Materials and Manufacturing Processes* 2018, *33* (15), 1701−1707.

(232) Ozcelik, B. K.; Ergun, C. Synthesis and characterization of iron oxide particles using spray pyrolysis technique. *Ceram. Int.* 2015, *41* (2, Part A), 1994−2005.

(233) Tischendorf, R.; Simmler, M.; Weinberger, C.; Bieber, M.; Reddemann, M.; Fröde, F.; Lindner, J.; Pitsch, H.; Kneer, R.; Tiemann, M.; Nirschl, H.; Schmid, H. J. Examination of the evolution of iron oxide nanoparticles in flame spray pyrolysis by tailored in situ particle sampling techniques. *Journal of Aerosol Science* 2021, *154*, 105722.

(234) Morales, M. P.; Bomati-Miguel, O.; Pérez de Alejo, R.; Ruiz-Cabello, J.; Veintemillas-Verdaguer, S.; O'Grady, K. Contrast agents

Shell Iron−Iron Oxide Nanoparticles Synthesized by Laser-Induced Pyrolysis. *Small* 2006, *2* (12), 1476−1483.

for MRI based on iron oxide nanoparticles prepared by laser pyrolysis. *Journal of Magnetism and Magnetic Materials* **2003**, *266* (1), 102−109.

(235) Thomas, G.; Boudon, J.; Maurizi, L.; Moreau, M.; Walker, P.; Severin, I.; Oudot, A.; Goze, C.; Poty, S.; Vrigneaud, J.-M.; Demoisson, F.; Denat, F.; Brunotte, F.; Millot, N. Innovative Magnetic Nanoparticles for PET/MRI Bimodal Imaging. *ACS Omega* **2019**, *4* (2), 2637−2648.

(236) Aime, S.; Cabella, C.; Colombatto, S.; Geninatti Crich, S.; Gianolio, E.; Maggioni, F. Insights into the use of paramagnetic Gd(III) complexes in MR-molecular imaging investigations. *Journal of Magnetic Resonance Imaging* **2002**, *16* (4), 394−406.

(237) Chan, K. W.-Y.; Wong, W.-T. Small molecular gadolinium-(III) complexes as MRI contrast agents for diagnostic imaging. *Coord. Chem. Rev.* **2007**, *251* (17), 2428−2451.

(238) Vuong, Q. L.; Berret, J.-F.; Fresnais, J.; Gossuin, Y.; Sandre, O. A Universal Scaling Law to Predict the Efficiency of Magnetic Nanoparticles as MRI T2-Contrast Agents. *Advanced Healthcare Materials* **2012**, *1* (4), 502−512.

(239) Osborne, E. A.; Jarrett, B. R.; Tu, C.; Louie, A. Y. Modulation of T2 Relaxation Time by Light-Induced, Reversible Aggregation of Magnetic Nanoparticles. *J. Am. Chem. Soc.* **2010**, *132* (17), 5934−5935.

(240) Ahmed, K.; Tabuchi, Y.; Kondo, T. Hyperthermia: an effective strategy to induce apoptosis in cancer cells. *Apoptosis* **2015**, *20* (11), 1411−1419.

(241) Kobayashi, T. Cancer hyperthermia using magnetic nano-particles. *Biotechnology Journal* **2011**, *6* (11), 1342−1347.

(242) Bi, Q.; Song, X.; Hu, A.; Luo, T.; Jin, R.; Ai, H.; Nie, Y. Magnetofection: Magic magnetic nanoparticles for efficient gene delivery. *Chin. Chem. Lett.* **2020**, *31* (12), 3041−3046.

(243) Chalasani, R.; Vasudevan, S. Cyclodextrin-Functionalized Fe3O4@TiO2: Reusable, Magnetic Nanoparticles for Photocatalytic Degradation of Endocrine-Disrupting Chemicals in Water Supplies. *ACS Nano* **2013**, *7* (5), 4093−4104.

(244) Chen, Z.; Yin, J.-J.; Zhou, Y.-T.; Zhang, Y.; Song, L.; Song, M.; Hu, S.; Gu, N. Dual Enzyme-like Activities of Iron Oxide Nanoparticles and Their Implication for Diminishing Cytotoxicity. *ACS Nano* **2012**, *6* (5), 4001−4012.

(245) Wang, L.; Shi, Y.; Zhang, H.; Bai, X.; Wang, Y.; Ma, T. Iron oxide nanostructures as highly efficient heterogeneous catalysts for mesoscopic photovoltaics. *Journal of Materials Chemistry A* **2014**, *2* (37), 15279−15283.

(246) Yang, H.-Y.; Rho, W.-Y.; Lee, S. K.; Kim, S. H.; Hahn, Y.-B. TiO2 Nanoparticles/Nanotubes for Efficient Light Harvesting in Perovskite Solar Cells. *Nanomaterials* **2019**, *9* (3), 326.

(247) Khalili Fard, J.; Jafari, S.; Eghbal, M. A. A Review of Molecular Mechanisms Involved in Toxicity of Nanoparticles. *Adv Pharm Bull* **2015**, *5* (4), 447−454.

(248) Shin, S. W.; Song, I. H.; Um, S. H. Role of Physicochemical Properties in Nanoparticle Toxicity. *Nanomaterials* **2015**, *5* (3), 1351−1365.

(249) Guo, H.; Zhang, J.; Boudreau, M.; Meng, J.; Yin, J.-j.; Liu, J.; Xu, H. Intravenous administration of silver nanoparticles causes organ toxicity through intracellular ROS-related loss of inter-endothelial junction. *Particle and Fibre Toxicology* **2015**, *13*, 21.

(250) Lehman, S. E.; Morris, A. S.; Mueller, P. S.; Salem, A. K.; Grassian, V. H.; Larsen, S. C. Silica nanoparticle-generated ROS as a predictor of cellular toxicity: mechanistic insights and safety by design. *Environmental Science: Nano* **2016**, *3* (1), 56−66.

(251) Kajita, M.; Hikosaka, K.; Iitsuka, M.; Kanayama, A.; Toshima, N.; Miyamoto, Y. Platinum nanoparticle is a useful scavenger of superoxide anion and hydrogen peroxide. *Free Radic Res* **2007**, *41* (6), 615−26.

(252) Zhang, L.; Laug, L.; Münchgesang, W.; Pippel, E.; Gösele, U.; Brandsch, M.; Knez, M. Reducing Stress on Cells with Apoferritin-Encapsulated Platinum Nanoparticles. *Nano Letters* **2010**, *10* (1), 219−223.

(253) Klem, M. T.; Mosolf, J.; Young, M.; Douglas, T. Photochemical Mineralization of Europium, Titanium, and Iron Oxy-

hydroxide Nanoparticles in the Ferritin Protein Cage. *Inorganic Chemistry* **2008**, *47* (7), 2237−2239.

(254) Moglia, I.; Santiago, M.; Soler, M.; Olivera-Nappa, A. Silver nanoparticle synthesis in human ferritin by photochemical reduction. *Journal of Inorganic Biochemistry* **2020**, *206*, 111016.

(255) Douglas, T.; Stark, V. T. Nanophase Cobalt Oxyhydroxide Mineral Synthesized within the Protein Cage of Ferritin. *Inorganic Chemistry* **2000**, *39* (8), 1828−1830.

(256) Wang, Z.; Huang, P.; Jacobson, O.; Wang, Z.; Liu, Y.; Lin, L.; Lin, J.; Lu, N.; Zhang, H.; Tian, R.; Niu, G.; Liu, G.; Chen, X. Biomineralization-Inspired Synthesis of Copper Sulfide−Ferritin Nanocages as Cancer Theranostics. *ACS Nano* **2016**, *10* (3), 3453−3460.

(257) Uchida, M.; Terashima, M.; Cunningham, C. H.; Suzuki, Y.; Willits, D. A.; Willis, A. F.; Yang, P. C.; Tsao, P. S.; McConnell, M. V.; Young, M. J.; Douglas, T. A human ferritin iron oxide nano-composite magnetic resonance contrast agent. *Magnetic Resonance in Medicine* **2008**, *60* (5), 1073−1081.

(258) Fantechi, E.; Innocenti, C.; Zanardelli, M.; Fittipaldi, M.; Falvo, E.; Carbo, M.; Shullani, V.; Di Cesare Mannelli, L.; Ghelardini, C.; Ferretti, A. M.; Ponti, A.; Sangregorio, C.; Ceci, P. A Smart Platform for Hyperthermia Application in Cancer Treatment: Cobalt-Doped Ferrite Nanoparticles Mineralized in Human Ferritin Cages. *ACS Nano* **2014**, *8* (5), 4705−4719.

(259) Li, H.; Zhang, W.; Ding, L.; Li, X.-W.; Wu, Y.; Tang, J.-H. Prussian blue-modified ferritin nanoparticles for effective tumor chemo-photothermal combination therapy via enhancing reactive oxygen species production. *Journal of Biomaterials Applications* **2019**, *33* (9), 1202−1213.

(260) Xu, N.; Yang, Y.-F.; Chen, L.; Lin, J. A Ferritin−Albumin−Cu Nanoparticle that Efficaciously Delivers Copper(II) Ions to a Tumor and Improves the Therapeutic Efficacy of Disulfiram. *ACS Omega* **2020**, *5* (18), 10415−10422.

(261) Yin, X.; Chen, B.; He, M.; Hu, B. Simultaneous determination of two phosphorylated p53 proteins in SCC-7 cells by an ICP-MS immunoassay using apoferritin-templated europium(III) and lutetium(III) phosphate nanoparticles as labels. *Microchimica Acta* **2019**, *186* (7), 424.

(262) Zhang, S.; Zang, J.; Chen, H.; Li, M.; Xu, C.; Zhao, G. The Size Flexibility of Ferritin Nanocage Opens a New Way to Prepare Nanomaterials. *Small* **2017**, *13* (37), 1701045.

(263) Dashtestani, F.; Ghourchian, H.; Najafi, A. Silver-gold-apoferritin nanozyme for suppressing oxidative stress during cryopreservation. *Materials Science and Engineering: C* **2019**, *94*, 831−840.

(264) Tosha, T.; Behera, R. K.; Theil, E. C. Ferritin ion channel disorder inhibits Fe(II)/O2 reactivity at distant sites. *Inorg Chem* **2012**, *51* (21), 11406−11.

(265) Zhang, Y.; Orner, B. P. Self-assembly in the ferritin nano-cage protein superfamily. *International journal of molecular sciences* **2011**, *12* (8), 5406−5421.

(266) Robertson, C. A.; Evans, D. H.; Abrahamse, H. Photodynamic therapy (PDT): A short review on cellular mechanisms and cancer research applications for PDT. *Journal of Photochemistry and Photobiology B: Biology* **2009**, *96* (1), 1−8.

(267) Allison, R. R.; Mota, H. C.; Bagnato, V. S.; Sibata, C. H. Bio-nanotechnology and photodynamic therapy—State of the art review. *Photodiagnosis and Photodynamic Therapy* **2008**, *5* (1), 19−28.

(268) Orth, K.; Rück, A.; Stanescu, A.; Beger, H. G. Intraluminal treatment of inoperable oesophageal tumours by intralesional photodynamic therapy with methylene blue. *Lancet* **1995**, *345* (8948), 519−20.

(269) Tang, W.; Xu, H.; Kopelman, R.; Philbert, M. A. Photo-dynamic characterization and in vitro application of methylene blue-containing nanoparticle platforms. *Photochem. Photobiol.* **2005**, *81* (2), 242−9.

(270) Yan, F.; Zhang, Y.; Kim, K. S.; Yuan, H.-K.; Vo-Dinh, T. Cellular uptake and photodynamic activity of protein nanocages

containing methylene blue photosensitizing drug. *Photochem. Photobiol.* 2010, 86, 662−666.

(271) Liu, X.; Wei, W.; Yuan, Q.; Zhang, X.; Li, N.; Du, Y.; Ma, G.; Yan, C.; Ma, D. Apoferritin−CeO2 nano-truffle that has excellent artificial redox enzyme activity. *Chemical Communications* 2012, 48 (26), 3155−3157.

(272) Wang, X.; Guo, Z. Towards the rational design of platinum(ii) and gold(iii) complexes as antitumour agents. *Dalton Transactions* 2008, 12, 1521−1532.

(273) Wheate, N. J.; Taleb, R. I.; Krause-Heuer, A. M.; Cook, R. L.; Wang, S.; Higgins, V. J.; Aldrich-Wright, J. R. Novel platinum(ii)-based anticancer complexes and molecular hosts as their drug delivery vehicles. *Dalton Transactions* 2007, No. 43, 5055−5064.

(274) Xing, R.; Wang, X.; Zhang, C.; Zhang, Y.; Wang, Q.; Yang, Z.; Guo, Z. Characterization and cellular uptake of platinum anticancer drugs encapsulated in apoferritin. *J. Inorg. Biochem.* 2009, 103, 1039−1044.

(275) Li, H.; Qian, Z. M. Transferrin/transferrin receptor-mediated drug delivery. *Med Res Rev* 2002, 22 (3), 225−50.

(276) Hemati Azandaryani, A.; Kashanian, S.; Derakhshandeh, K. Folate Conjugated Hybrid Nanocarrier for Targeted Letrozole Delivery in Breast Cancer Treatment. *Pharm. Res.* 2017, 34 (12), 2798−2808.

(277) Khoshnejad, M.; Parhiz, H.; Shuvaev, V. V.; Dmochowski, I. J.; Muzykantov, V. R. Ferritin-based drug delivery systems: Hybrid nanocarriers for vascular immunotargeting. *J. Controlled Release* 2018, 282, 13−24.

(278) Katti, G.; Ara, S. A.; Shireen, A. Magnetic resonance imaging (MRI) - A review. *Int. J. Dental Clin.* 2011, 3 (1), 65−70.

(279) Rogosnitzky, M.; Branch, S. Gadolinium-based contrast agent toxicity: a review of known and proposed mechanisms. *BioMetals* 2016, 29 (3), 365−376.

(280) Ramalho, J.; Semelka, R. C.; Ramalho, M.; Nunes, R. H.; AlObaidy, M.; Castillo, M. Gadolinium-Based Contrast Agent Accumulation and Toxicity: An Update. *American Journal of Neuroradiology* 2016, 37 (7), 1192.

(281) Raynal, I.; Prigent, P.; Peyramaure, S.; Najid, A.; Rebuzzi, C.; Corot, C. Macrophage endocytosis of superparamagnetic iron oxide nanoparticles: mechanisms and comparison of ferumoxides and ferumoxtran-10. *Invest Radiol* 2004, 39 (1), 56−63.

(282) Yancy, A. D.; Olzinski, A. R.; Hu, T. C.; Lenhard, S. C.; Aravindhan, K.; Gruver, S. M.; Jacobs, P. M.; Willette, R. N.; Jucker, B. M. Differential uptake of ferumoxtran-10 and ferumoxytol, ultrasmall superparamagnetic iron oxide contrast agents in rabbit: critical determinants of atherosclerotic plaque labeling. *J Magn Reson Imaging* 2005, 21 (4), 432−42.

(283) Cai, Y.; Wang, Y.; Xu, H.; Cao, C.; Zhu, R.; Tang, X.; Zhang, T.; Pan, Y. Positive magnetic resonance angiography using ultrafine ferritin-based iron oxide nanoparticles. *Nanoscale* 2019, 11 (6), 2644−2654.

(284) Charlton, J. R.; Pearl, V. M.; Denotti, A. R.; Lee, J. B.; Swaminathan, S.; Scindia, Y. M.; Charlton, N. P.; Baldelomar, E. J.; Beeman, S. C.; Bennett, K. M. Biocompatibility of ferritin-based nanoparticles as targeted MRI contrast agents. *Nanomedicine: Nanotechnology, Biology and Medicine* 2016, 12 (6), 1735−1745.

(285) Aime, S.; Frullano, L.; Geninatti Crich, S. Compartmentalization of a gadolinium complex in the apoferritin cavity: A route to obtain high relaxivity contrast agents for magnetic resonance imaging. *Angew. Chem., Int. Ed.* 2002, 41, 1017−1019.

(286) Uchida, M.; Kang, S.; Reichhardt, C.; Harlen, K.; Douglas, T. The ferritin superfamily: Supramolecular templates for materials synthesis. *Biochimica et Biophysica Acta (BBA) - General Subjects* 2010, 1800 (8), 834−845.

(287) Okuda, M.; Iwahori, K.; Yamashita, I.; Yoshimura, H. Fabrication of nickel and chromium nanoparticles using the protein cage of apoferritin. *Biotechnol. Bioeng.* 2003, 84 (2), 187−194.

(288) Yamashita, I.; Iwahori, K.; Kumagai, S. Ferritin in the field of nanodevices. *Biochimica et Biophysica Acta (BBA) - General Subjects* 2010, 1800 (8), 846−857.

(289) Miura, A.; Tsukamoto, R.; Yoshii, S.; Yamashita, I.; Uraoka, Y.; Fuyuki, T. Non-volatile flash memory with discrete bionanodot floating gate assembled by protein template. *Nanotechnology* 2008, 19 (25), 255201.

(290) Okuda, M.; Yamashita, I.; Iwahori, K.; Yoshimura, H. Fabrication of In2O3 Oxide Semiconductor Nano-Particles Using Apoferritin. *MRS Proc.* 2005, 873, 313.

(291) Yamashita, I.; Kirimura, H.; Okuda, M.; Nishio, K.; Sano, K.; Shiba, K.; Hayashi, T.; Hara, M.; Mishima, Y. Selective nanoscale positioning of ferritin and nanoparticles by means of target-specific peptides. *Small* 2006, 2 (10), 1148−52.

(292) Matsukawa, N.; Nishio, K.; Sano, K.; Shiba, K.; Yamashita, I. Hexagonal close-packed array formed by selective adsorption onto hexagonal patterns. *Langmuir* 2009, 25 (6), 3327−30.

(293) Takagi, D.; Yamazaki, A.; Otsuka, Y.; Yoshimura, H.; Kobayashi, Y.; Homma, Y. Gold-filled apo-ferritin for investigation of single-walled carbon nanotube growth on substrate. *Chemical Physics Letters - CHEM PHYS LETT* 2007, 445, 213−216.

(294) Kumagai, S.; Ono, T.; Yoshii, S.; Kadotani, A.; Tsukamoto, R.; Nishio, K.; Okuda, M.; Yamashita, I. Position-Controlled Vertical Growths of Individual Carbon Nanotubes Using a Cage-Shaped Protein. *Appl. Phys. Exp.* 2010, 3, 015101.

(295) Colton, J. S.; Erickson, S. D.; Smith, T. J.; Watt, R. K. Sensitive detection of surface- and size-dependent direct and indirect band gap transitions in ferritin. *Nanotechnology* 2014, 25 (13), 135703.

(296) Smith, T. J.; Erickson, S. D.; Orozco, C. M.; Fluckiger, A.; Moses, L. M.; Colton, J. S.; Watt, R. K. Tuning the band gap of ferritin nanoparticles by co-depositing iron with halides or oxo-anions. *Journal of Materials Chemistry A* 2014, 2 (48), 20782−20788.

(297) Pekarik, V.; Peskova, M.; Guran, R.; Novacek, J.; Heger, Z.; Tripsianes, K.; Kumar, J.; Adam, V. Visualization of stable ferritin complexes with palladium, rhodium and iridium nanoparticles detected by their catalytic activity in native polyacrylamide gels. *Dalton Transactions* 2017, 46 (40), 13690−13694.

(298) Kumari, S.; Häring, M.; Gupta, S. S.; Díaz Díaz, D. Catalytic Macroporous Biohydrogels Made of Ferritin-Encapsulated Gold Nanoparticles. *ChemPlusChem* 2017, 82 (2), 225−232.

(299) Peskova, M.; Ilkovics, L.; Hynek, D.; Dostalova, S.; Sanchez-Carnerero, E. M.; Remes, M.; Heger, Z.; Pekarik, V. Detergent-modified catalytic and enzymomimetic activity of silver and palladium nanoparticles biotemplated by Pyrococcus furiosus ferritin. *J. Colloid Interface Sci.* 2019, 537, 20−27.

(300) Keyes, J. D.; Hilton, R. J.; Farrer, J.; Watt, R. K. Ferritin as a photocatalyst and scaffold for gold nanoparticle synthesis. *J. Nanopart. Res.* 2011, 13, 2563−2575.

(301) Saenz, N.; Sanchez, M.; Galvez, N.; Carmona, F.; Arosio, P.; Dominguez-Vera, J. M. Insights on the (Auto)Photocatalysis of Ferritin. *Inorg. Chem.* 2016, 55, 6047−6050.

(302) Cornell, T. A.; Orner, B. P. Medium throughput cage state stability screen of conditions for the generation of gold nanoparticles encapsulated within a mini-ferritin. *Bioorg. Med. Chem.* 2018, 26 (19), 5253−5258.

(303) Rafipour, R.; Kashanian, S.; Hashemi, S.; Shahabadi, N.; Omidfar, K. An electrochemical biosensor based on cobalt nano-particles synthesized in iron storage protein molecules to determine ascorbic acid. *Biotechnology and applied biochemistry* 2016, 63 (5), 740−745.

(304) Xu, N.; Yang, Y.-F.; Chen, L.; Xu, L.; Xu, X.-J.; Lin, J. Enhancing the Effect of Pharmacological Ascorbate in Cancer Therapy via Acid-Triggered Ferritin Nanoparticles. *Advanced Biosystems* 2019, 3 (5), 1900006.

(305) Zang, J.; Zheng, B.; Zhang, X.; Arosio, P.; Zhao, G. Design and site-directed compartmentalization of gold nanoclusters within the intrasubunit interfaces of ferritin nanocage. *J. Nanobiotechnol.* 2019, 17, 79.

(306) Zhang, T.; Cao, C.; Tang, X.; Cai, Y.; Yang, C.; Pan, Y. Enhanced peroxidase activity and tumour tissue visualization by cobalt-doped magnetoferritin nanoparticles. *Nanotechnology* 2017, 28 (4), 045704.

(307) Okuda, M.; Kobayashi, Y.; Suzuki, K.; Sonoda, K.; Kondoh, T.; Wagawa, A.; Kondo, A.; Yoshimura, H. Self-Organized Inorganic Nanoparticle Arrays on Protein Lattices. *Nano Letters* **2005**, *5* (5), 991−993.

(308) Song, N.; Zhang, J.; Zhai, J.; Hong, J.; Yuan, C.; Liang, M. Ferritin: A Multifunctional Nanoplatform for Biological Detection, Imaging Diagnosis, and Drug Delivery. *Acc. Chem. Res.* **2021**, *54* (17), 3313−3325.